

A
PROJECT REPORT
ON
**ANALYSIS OF PAVEMENTS FOR FLUCTUATING
DYNAMIC LOADS**

SUBMITTED IN PARTIAL FULFILLMENT OF THE REQUIREMENTS
FOR THE AWARD OF THE DEGREE

OF
MASTER OF TECHNOLOGY
IN
GEOTECHNICAL ENGINEERING

Submitted by
Shagun

2k19/GTE/12

Under the supervision of
Professor Ashutosh Trivedi



DEPARTMENT OF CIVIL ENGINEERING
DELHI TECHNOLOGICAL UNIVERSITY

(Formerly Delhi College of Engineering)

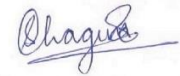
Bawana Road, Delhi – 110042

OCTOBER 2021

DELHI TECHNOLOGICAL UNIVERSITY
(Formerly Delhi College of Engineering)
Bawana Road, Delhi – 110092

CANDIDATE’S DECLARATION

I, **SHAGUN**, roll no. **2k19/GTE/12** student of M.Tech, Geotechnical Engineering, hereby declare that the Dissertation titled “**Analysis of Pavements for Fluctuating Dynamic Loads**” which is submitted by me to the Department of Civil Engineering, Delhi Technological University, Delhi in partial fulfillment of the requirement for the award of the Master of Technology is original and not copied from any source without proper citation. This is an authentic record of my work carried out under the supervision of Prof. Ashutosh Trivedi. This work has not been previously formed the basis for the award of any Degree, Diploma Associateship, Fellowship, or any other similar title or recognition.



(SHAGUN)

Place: Delhi

Date: 15/10/2021

DEPARTMENT OF CIVIL ENGINEERING

DELHI TECHNOLOGICAL UNIVERSITY

(Formerly Delhi College of Engineering)

Bawana Road, Delhi – 110092

CERTIFICATE

I hereby certify that the Project Dissertation titled “**Analysis of Pavements for Fluctuating Dynamic Loads**” which is submitted by SHAGUN, roll no. 2k19/GTE/12 (Civil Engineering), Delhi Technological University, Delhi in the partial fulfillment of the requirement for the award of the degree of Master of Technology, is a record of the project work carried out by the student under my supervision. To the best of my knowledge, this work has not been submitted in part or full for any degree or diploma to this University or elsewhere.

Place: Delhi

Date: 15/10/2021

(Prof. Ashutosh Trivedi)

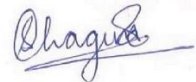
SUPERVISOR

ACKNOWLEDGEMENT

I express my profound gratitude to Prof. Ashutosh Trivedi, Department of Civil Engineering, Delhi Technological University, whose guidance, and words of encouragement have been a great force that enabled me to prepare this project report on the topic “**Analysis of Pavements for Fluctuating Loads**”. He devoted considerable time to guide me through the work and simultaneously checking on the work and making valuable suggestions. His guidance helped me to write this thesis and overcome all the obstacles I encountered during the work.

I also express my gratitude towards Ph.D. scholar, Mr. Yakshansh Kumar, Delhi Technological University for helping me and correcting my work. He made valuable suggestions to improve my project work.

I would like to thank my parents for constantly encouraging me and being my support system throughout the work. I am also thankful to the faculties and staff of Delhi Technological University for providing me with facilities that helped me to carry out the project work.



SHAGUN
(2k19/GTE/12)

ABSTRACT

Pavement health is affected by factors such as the pavement material, fluctuating loads, and vehicle weight. This study aims to understand the dynamic behavior of fluctuating loads on the pavement life and service. The study takes into consideration the frequency generated by different vehicles. The vehicles are classified as per IRC 37 -2018 and then further classified based on the axle configuration. The finite element analysis using Abaqus is carried out in which a flexible pavement is modeled. RPM value, axle configuration, and gross vehicle weight of different commercial and domestic vehicles are taken for the study. It's been seen that with increasing frequency (or RPM) the wavelength of pavement roughness decreases and with an increase in velocity the wavelength increases. The vehicle speed and gross weight play a major role in inducing the stresses on the pavement. As the frequency increased and load decreased, the stress value decreased. It means that the stress is more when the load is higher, and frequency is low. The wavelength of pavement roughness decreases with an increase in frequency but increases with speed increases.

CONTENT

Declaration	ii
Certificate	iii
Acknowledgment	iv
Abstract	v
List of Tables	viii
List of Figures	ix
Chapter 1 Introduction	1
1.1 Overview	1
1.2 Mechanism of load – pavement interaction	2
1.3 Dynamic analysis of load – pavement interaction	3
1.4 Types of pavements	3
1.5 Finite element analysis	4
1.6 Objectives	6
Chapter 2 Literature Review	7
2.1 General	7
2.2 Research gap	14
Chapter 3 Materials and Methodology	15
3.1 Introduction to dynamic loads	15
3.2 Vehicle classification	15
3.3 Pavement and material properties	18
3.4 Dynamic formulae	19
3.5 Application of soil dynamics	21
3.6 Finite element method	21
3.7 Steady-state dynamics analysis	22
3.8 Assumptions	22
3.9 Modelling method	23
3.10 Model dimensions	24
3.12 Meshing	25
3.13 Load and boundary conditions	26
3.13.1 Boundary conditions	26
3.13.2 Loads	26

Chapter – 4 Result and discussion	28
4.1 Dynamic model validation	28
4.2 Dynamic model analysis	31
4.2.1 Effect of speed on pavement stress intensity	31
4.2.1.1 When the speed of the vehicle is 20 kmph	31
4.2.1.2 When the speed of the vehicle is 40 kmph	34
4.2.1.3 When the speed of the vehicle is 60 kmph	37
4.2.2 Maximum stress due to velocity	39
4.2.3 Stress variation due to frequency in the pavement layers	40
4.2.3.1 Effect of frequency of vehicle having load 18500 kg (18.5 tonnes)	40
4.2.3.2 Effect of frequency of vehicle having load 42000 kg (42 tonnes)	43
4.2.3.3 Effect of frequency of vehicle having load 1335 kg (1.335 tonnes)	46
4.2.3.4 Effect of frequency of vehicle having load 1600 kg (1.6 tonnes)	48
4.3 Pavement roughness	51
Chapter – 5 Conclusion and future scope	52
5.1 Conclusion	52
5.2 Future scope	53
References	54

LIST OF TABLES

Table 1 – Classification of domestic vehicle	16
Table 2 – Classification of commercial vehicles	17
Table 3 – Types of commercial vehicles having GVW = 18500 kg and axle = 2	17
Table 4 – Types of commercial vehicles having GVW = 42000 kg and axle = 5	17
Table 5 – Classification of domestic vehicles having GVW = 1335 kg and axle = 2	18
Table 6 – Classification of domestic vehicles having GVW = 1600 to 1700 kg and axle = 2	18
Table 7 – Material properties	19
Table 8 – Wavelength of pavement roughness due to various velocities of different vehicle types	20
Table 9 – Pavement model dimensions	24
Table 10 – Value of load and amplitude used in the modeling	27
Table 11 – Damping parameters	28
Table 12 – Design parameters	28
Table 13 – Maximum stress intensity at different nodes	30
Table 14 – Maximum stress at different velocities and nodes	39
Table 15 – Stress variation due to the given frequency for 18500 kg vehicle load	41
Table 16 – Stress variation due to the given frequency for 42000 kg vehicle load	43
Table 17 – Stress variation due to the given frequency for 1335 kg vehicle load	46
Table 18 – Stress variation due to the given frequency for 1600 kg vehicle load	48

LIST OF FIGURES

Figure 1 – Role of load pavement interaction in various applications	2
Figure 2 – Layers of flexible pavement	4
Figure 3 – Layers of rigid pavement	4
Figure 4 – Classification of vehicles	16
Figure 5 – A systematic model of flexible pavement layers used in modeling	18
Figure 6 – Wheel load acting on the pavement	19
Figure 7 – Flow chart of the numerical analysis	23
Figure 8 – Systematic view of flexible pavement modeled in ABAQUS	24
Figure 9 – 8 – Node brick element mesh	25
Figure 10 - Meshing in the model	25
Figure 11 – Load application (shown by red downward arrows)	27
Figure 12 – Sectional view and nodes along the YZ plane	29
Figure 13 – Stress contour for the model at velocity 12.5 m/s	30
Figure 14 – Stress intensity at different nodes	31
Figure 15 – Dynamic stress contour at velocity 5.55 m/s	32
Figure 16 – Stress variation due to velocity 20 kmph in bitumen layer	32
Figure 17 – Stress variation due to velocity of 20 kmph in the subbase layer	33
Figure 18 – Stress variation due to velocity 20 kmph in the subgrade layer	33
Figure 19 – Dynamic stress contour at velocity 11.11 m/s	34
Figure 20 – Stress variation due to velocity 40 kmph in bitumen layer	35
Figure 22 – Stress variation due to velocity 40 kmph in the subgrade layer	36
Figure 23 – Dynamic stress contour at velocity 16.67 m/s	37
Figure 24 – Stress variation due to velocity 60 kmph in bitumen layer	37
Figure 25 – Stress variation due to velocity of 60 kmph in the subbase layer	38
Figure 26 – Stress variation due to velocity 60 kmph in the subgrade layer	38
Figure 27 – Maximum stress at different nodes	40
Figure 28 – Stress variation in bitumen layer for a vehicle load of 18500 kg	41
Figure 29 – Stress variation in the subbase layer for a vehicle load of 18500 kg	42
Figure 30 – Stress variation in subgrade layer for a vehicle load of 18500 kg	42
Figure 31 – Stress variation in bitumen layer for a vehicle load of 42000 kg	44
Figure 32 – Stress variation in the subbase layer for a vehicle load of 42000 kg	44

Figure 33 – Stress variation in subgrade layer for a vehicle load of 42000 kg	45
Figure 34 – Stress variation in bitumen layer for a vehicle load of 1335 kg	46
Figure 35 – Stress variation in the subbase layer for a vehicle load of 1335 kg	47
Figure 36 – Stress variation in subgrade layer for a vehicle load of 1335 kg	47
Figure 37 – Stress variation in bitumen layer for a vehicle load of 1600 kg	49
Figure 38 – Stress variation in the subbase layer for a vehicle load of 1600 kg	49
Figure 39 – Stress variation in subgrade layer for a vehicle load of 1600 kg	50
Figure 40 - Wavelength of pavement roughness at a different velocity	51

CHAPTER -1

INTRODUCTION

1.1 Overview

Roads are a major mode of transportation all over the world. Therefore, it is necessary to design and construct a sturdy and high-quality pavement for the easy and smooth movement of vehicles. The study of the dynamic response of load – pavement interaction has received a lot of attention by researchers (Jianhong 2020, Hao Wang 2020, Wang 2020, Assogba et al. 2019, Geonaga et al. 2018, Kadela 2016, Beskou and Theodorakopoulos 2011, Kim et al 2009, Mulungye et al. 2006) over the past few years because of the relevance in designing of the pavement structure.

The primary function of the pavement is to transfer the load from the vehicles to the soil subgrade layer. Hence it is important to study the various types of loads that affect pavement serviceability and the stresses generated by them. These stresses are produced due to the continuous movement of the different types of vehicles such as domestic or commercial vehicles. The load of the vehicles and their speed are a few of the contributing factors which affect the pavement performance. (Justo, 2011)

The following parameters characterize the loads and vehicles forces experienced by the pavement

- i. Tire loads
- ii. Axle and tire configuration
- iii. Repetition of loads
- iv. Distribution of load across pavement
- v. Vehicle speed

In comparison with other static structures, the loads on the pavement structure are mobile and dynamic. The load experienced keeps changing from point to point because of the pavement surface roughness and the vibrations produced by the vehicle itself. Scholars and researchers (Hao Wang 2020, Wang 2020, Assogba et al. 2019, Tang et al. 2020, Geonaga et al. 2018, Li et al. 2018, Kadela 2016, Beskou and Theodorakopoulos

2011, Kim et al. 2009, Mulungye et al. 2006) have experimented and study the effect of dynamic loads on the pavement.

The geometry and mechanical properties of the pavement layers control the stress-strain induced in the pavement by the contact stresses. Vehicle–pavement interaction is an integral part not only of pavement design but also has an impact on infrastructure management, vehicle suspension design, and transportation economy. Vehicle–pavement interaction has a huge economic impact (Figure – 1). Due to the constant movement of dynamic loads, the service life of the pavement eventually deteriorates. The surface becomes uneven and rougher, the operation cost of vehicles increases, and also the maintenance cost of the roads increases.

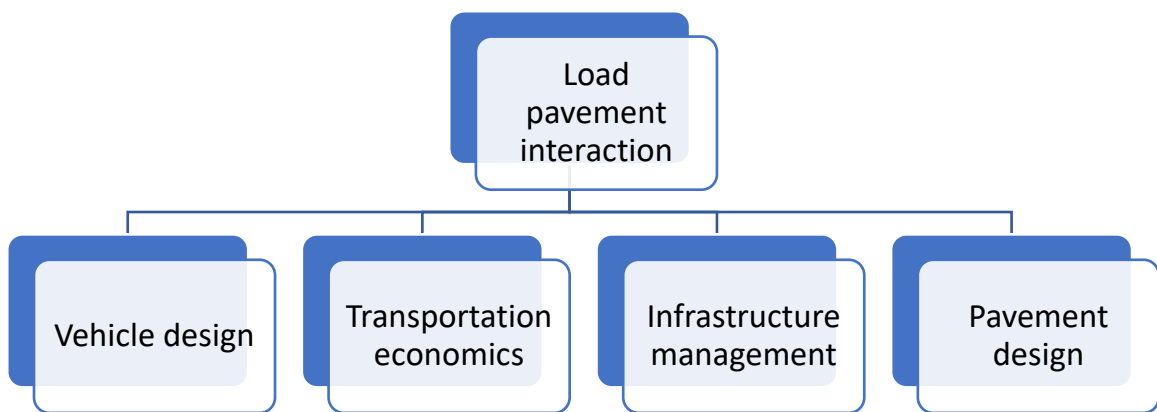


Figure 1 – Role of load pavement interaction in various applications

1.2 Mechanism of load – pavement interaction

As the vehicle moves on the road, dynamic loads are induced on the pavement. The loads from the vehicle are transferred to the pavement through the tires; hence the contact stresses on the pavement surface and the geometry of the loaded area are affected by the tire type and inflation pressure. (Khavassefat, 2014)

In general, forces are imposed on both pavement and vehicles via each other through the process of deterioration of pavement surface by the application of loads, which leads to excitation of axle suspensions resulting from increased surface roughness under a moving vehicle and resulting in more dynamic loads on the pavement surface. The process is accelerating, where variations in pavement condition and vehicle load reinforce each other through time, which ultimately becomes more significant as the pavement deteriorates.

1.3 Dynamic analysis of load – pavement interaction

In the analysis when pavement surface unevenness is considered, the result of vehicle interaction with the pavement is a dynamic process. The dynamic loads are assumed to increase the pavement damage. Therefore, the dynamic effects of load–pavement interaction has a very significant influence on the stresses induced in the various pavement layers. (Dae-Wook Park, 2014)

The dynamic interaction between the load and pavement is taken into account by considering the vehicle load and pavement as an integrated store. One of the important parameters that affect the stresses induced on the pavement due to dynamic load is the speed of the vehicle and also the traffic flow. (Wang, 2020)

1.4 Types of Pavements

The pavement carries the load on its top surface which is transferred as stress through the subsequent layers to the subgrade. The stresses transferred to the subgrade layer are comparatively lower than the contact pressure under the wheel load of the vehicle pavement interaction (Justo, 2011). It is important to design a well-constructed pavement so that the pavement elastic deformation is within the permissible limits.

Based on structural behavior, the pavement is classified as-

- i. **Flexible pavement** – The flexible pavements under load application have flexible structural action and have low flexural strength. The flexible pavement typically consists of 4 layers, namely, surface course, base course, subgrade course, and subgrade course (Figure 2). The load transfer through the layers in flexible pavement takes place through the grain-to-grain transfer of the point of contact in the granular structure. The best flexible pavement material is bituminous concrete. According to the **layer system concept**, the flexible pavement can be constructed in layers and the top layer has to be the strongest as the highest compressive strength is ensured by the top layer only. The lower layers take up the lesser magnitudes of the stresses. The flexible pavements are designed using the empirical design charts and equations taking into account the design factors (Justo, 2011).
- ii. **Rigid pavement** – The rigid pavements have not able flexural strength. The transfer of loads doesn't take place through grain-to-grain transfer. The rigid pavement has

slab action which transfers the load to a wider area in subsequent layers. The main structural difference between the rigid pavement and flexible pavement is that the critical condition of stress in the rigid pavement is the maximum flexural stress occurring in the slab due to wheel load and temperature changes (Justo, 2011). The rigid pavement consists of 3 layers: cement concrete slab, base course, and soil subgrade (Figure 3). The design of rigid pavement is done using the elastic theory and stresses are analyzed using the same theory, where it is assumed that the pavement is resting over an elastic or viscous foundation.

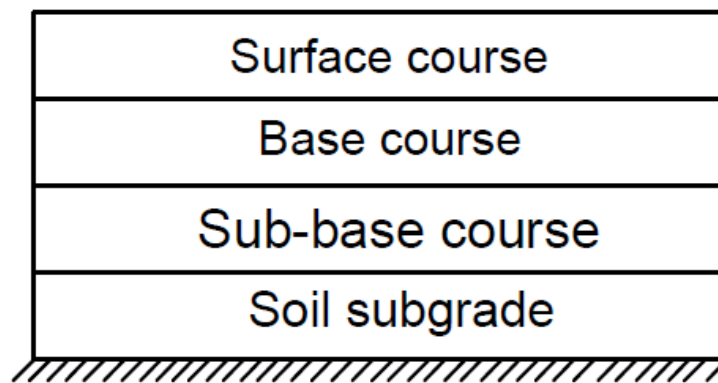


Figure 2 – Layers of flexible pavement

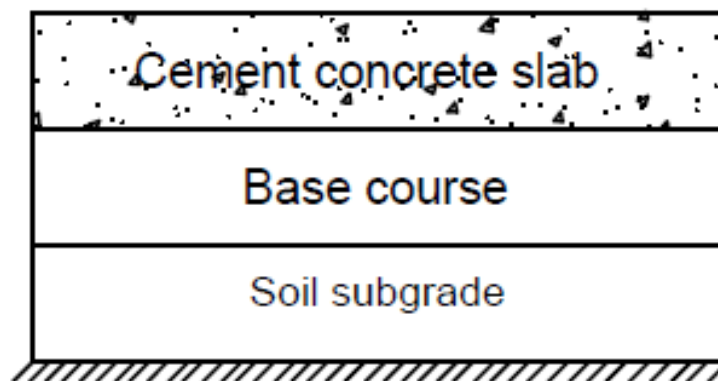


Figure 3 – Layers of rigid pavement

1.5 Finite element analysis

The finite element analysis is numerical technique-based analysis. This method deals with the problem complexities such as boundary conditions, geometry, and load variation. This is a very flexible tool for studying and analyzing a problem. The different software that uses the finite element analysis is Staad-Pro, Ansys, and Abaqus, etc. The need for finite element analysis came to light as a means of doing stress analysis. The

method was used to solve the problems related to the matrix method in solid mechanics. But with time and advancement in technology, the application field of finite element analysis expanded to fluid dynamics, soil mechanics, heat transfer, etc. (Bhavikatti, 2005). One can perform static as well as dynamic analysis using the finite element analysis

In the finite element method, the number of unknowns is reduced from infinite to finite unknowns by splitting the problem area into smaller parts known as elements. After identifying and selecting the elements, the next step is to assign the properties to those elements. The purpose of assigning the element properties is to get the structural properties. The boundary conditions are set after assigning the material properties. The nodal unknowns found from the solution of the equation are used to calculate the values of strain, stress, etc. (Gouri Dhatt, 2012)

The steps in carrying out finite element analysis are –

- i. Elements and variables selection
- ii. Selection of interpolation functions
- iii. Finding the element properties
- iv. Assembling of element properties to know the global properties
- v. Imposition of boundary conditions
- vi. Determination of nodal unknowns by solving the system equations
- vii. Using the nodal unknowns in the calculation to get the required values

The different analysis that can be done using the finite element method is linear or non – linear analysis, static analysis, dynamic analysis, thermal analysis, fluid analysis, electromagnetic analysis, heat transfer, etc. It is very important to identify the type of analysis to be carried out because the analysis type defines the outcome.

The basic/main steps in the finite element analysis are

- **Pre-processing** – In this step the geometry, material properties, assembling, boundary conditions, load, etc. are defined. The meshing is defined by the software only, but the density and size of the mesh are user-defined. The analysis type is decided before carrying the process. The data used must be reviewed beforehand.
- **Numerical analysis** – Matrix is generated by the software itself by the material properties defined in pre-processing. These matrices are then combined to form one

large matrix for the system which then determines the field nodal values using the system equations.

- **Post-processing** – The result obtained from the numerical analysis is then displayed in graphical form. This is an automatic step, and the analyst determines what results must be displayed.

1.6 Objectives

- To understand the frequency effect of the pavement undulations as a measure of the roughness.
- To study the effect of vehicle speed on the pavement.
- To understand the effect of speed along with the pavement profiles.
- To study the effect of frequency on the stress intensity response of the pavement.
- To study how the gross vehicle weight affects the stress variation in the pavement.
- To understand the effect of the axle on the pavement response.

CHAPTER - 2

LITERATURE REVIEW

2.1 General

The frequency and vehicle speed effect on pavement response has been analyzed and examined by various researchers using finite element method and experimental procedures. The literature review is presented below

Zhao and Wang (2020) studied and analyzed the dynamic response of the pavement by inducing a load of various trucks using the 3-dimensional finite element method. The key area of study was the pavement response due to harmonic excitation and see how the pavement roughness affects the variation of dynamic load and pavement response. An impulse response method was used to calculate the flexible pavement response subjected to dynamic loads. The field results were by the calculated results. The pavement dynamic response kept varying at different points on the pavement owing to the surface roughness. The failure of the pavement was concluded at the location where greater tensile stress was induced. The load frequency was found to be insignificant for the pavement response under dynamic loads.

Jianhong (2020) used the finite element method software Ansys for developing and analyzing a 3D asphalt pavement model. The stress intensity time history curve of the pavement was obtained under the fluctuating loads. The stress intensity response laws under fluctuating loads were analyzed for providing a reference for the stress intensity conditions under dynamic loads. The study concluded that irrespective of the point on the pavement, the stress intensity time history curve fluctuated frequently under the fluctuating load. It means that the dynamic load influence on the pavement dynamic response is complex.

Zhang et al. (2020) studied the pavement response due to the frequency and magnitude of vehicle dynamic loads. The frequency and magnitude of the dynamic loads are dependent on the axle configuration, pavement surface roughness, and vehicle speed. The vertical tire forces caused by different pavement surface roughness profiles were studied and estimated using full truck models. The different pavement

responses under dynamic loads were simulated using the advanced 3-dimensional finite element method. The cumulative probability distribution and dynamic load coefficient (DLC) were used to assess the variation in dynamic loads. The pavement response was predicted using numerical simulations based on vehicle speed, pavement roughness, and dynamic loads. Following the analysis, it was determined that a rougher pavement surface causes greater pavement responses and accelerates pavement failure at locations where high dynamic loads have been induced. Higher speeds in general induce minor strain reactions in asphalt pavement. Under dynamic loads on rough pavements, however, the effect of vehicle speed on pavement response becomes less visible.

Tang et. al. (2020) carried out the analysis using BIM and finite element method software. The purpose of this research was to develop a data conversion interface based on BIM and Abaqus. The constructed parameterized model and data conversion interface were used in the structural study of semi-rigid base asphalt pavement. The construction design plan and structural analysis were two distinct phases in conventional pavement design. The data conversion interface successfully transferred data to the BIM model, according to the findings. Vertical compressive strain, Mises stress, and tensile strain were the three parameters calculated at the bottom of the asphalt layer during the research.

Goenaga et. al. (2019) studied the effect of dynamic loads induced by the pavement roughness on the specific locations of the pavement. For all pavement profiles, the dynamic load produced at the tire pavement interface was calculated. Each profile's International Roughness Index (IRI) and Dynamic Load Index (DLI) were calculated. The influence of road roughness and vehicle speed on the dynamic load was investigated using longitudinal pavement profiles. According to the observations, pavement roughness is the main factor that causes dynamic stresses at the tire pavement interface, for a given speed. As the vehicle speed and pavement roughness increased, the dynamic loads fluctuated more. In addition, a new measure called the Traffic Correction Factor (TCF) was developed to account for the effects of both roughness and vehicle speed on dynamic load.

Assogba et. al. (2019) studied the damage done to the pavement due to poor designing and construction and the increase in traffic loads and dynamic load due to the heavy trucks. The research focuses on modeling the key stress-strain response at the asphalt pavement's bottom under various load weights and vehicle speeds. The pavement's transient dynamic study was studied using a large-scale 3D viscoelastic finite element model. Under heavy truck moving loads, the reaction time of longitudinal, vertical, and shearing stress-strain at the bottom layer of the asphalt pavement comprises both a tensile and compressive component, according to this study. In addition, as the vehicle speed was reduced, the load duration on the pavement increased, and the shock effect caused by the vehicle load was intensified. It was also discovered that axle weight had an impact on pavement deterioration.

Li et. al. (2018) determined the dynamic frequency of the pavement subjected to vehicle loading using the Mechanistic-Empirical Pavement Design Guide (MEPDG) which employs the equivalent thickness concept and the 45° tie diffusion approach. To determine the pavement dynamic response, the installation of the strain gauges was done on the pavement. Dynamic response data were collected for various vehicle loadings and speeds. The dynamic frequency of asphalt pavement under live vehicle loads was examined from a spectral perspective applying the Fast Fourier Transform (FFT) approach. According to the findings, the representative frequency increases with increasing speed and decreases with increasing loading magnitude and temperature. MEPDG's method overestimates the frequency of asphalt pavements.

Kadela (2016) studied the pavement response due to the heavy vehicle load. This was important to study as a structure's durability requirement is met only when it performs its function in terms of load-bearing capacity, serviceability, and stability without incurring additional costs. As the number of vehicles increased on the road, the load intensity per wheel increased too. The maximum vertical displacement increases in proportion to the thickness of the pavement. The obtained displacement and strain response values of the pavement–subgrade system were alike, however, the analyzed values varied according to the continuous model used. During the research, the highest value of horizontal strain was yielded by the axially symmetric model on the subgrade top surface.

Wu et. al (2014) used finite element software Abaqus to study the concrete pavement with an asphalt isolating layer dynamic response under moving loads. The analysis showed that the stresses and deflection of the concrete slab were proportional to the slab thickness. In this paper, the moving loads were taken as surface loads that had specific speeds. The stress and deflection were calculated at critical points on the pavement by changing the pavement thickness. The results showed that the stress and deflection were dependent on the thickness of the isolating layer but not on the modulus of the isolating layer.

Lin (2014) studied the spectral approach for understanding the variations of the dynamic loads moving with a constant speed on the pavement. As the vehicle speed varied, the roughness of the pavement and dynamic loading varied too. A quarter truck model was adopted as the study model in this study. The load spectrum was calculated using random vibration theory, and the variance in dynamic vehicle load was calculated. The effects of vehicle speed and road roughness on dynamic vehicle load variation were studied.

Beskou and Theodorakopoulos (2011) studied the dynamic response of the loads moving on the pavement surface. The foundation soil was modeled as a system of elastic springs, while the pavement was modeled as a beam or plate. With varying or constant time and vehicle speed, the loads were considered to vary or remain constant. The pavement's dynamic response was investigated using linear elastic material behavior. Analytical, numerical, and mathematical approaches were used in the analysis. The effect of load fluctuation with velocity on pavement service had been documented. The structure and stress-experienced behavior of the pavement was heavily influenced by its thickness and material qualities.

Rahman et. al. (2011) designed the pavement model using finite element software Abaqus in which the dimensions of the model, types of element, and methods of meshing were taken by trial and error. To identify the damage due to the tire imprint, the shape of the contact area was considered. The tire impression area should be rectangular with two semi-circles on both sides, according to the findings reported in this research. Other shape contact regions are unsuitable because they produce fewer stresses and strains per unit of area. It has been discovered that varying contact pressure causes a 30% increase in stress. For pressure that varies spatially, the strain

value does not change dramatically. As a result, uniform contact pressure does not affect the outcome when a strain, fatigue, or permanent deformation are included in the design criteria for wheel load application.

Barbosa (2011) focused on developing a spectral method for obtaining the frequency response of a half-vehicle in the frequency domain when it is subjected to observed pavement roughness. The methodology presented in the paper was based on the modal vehicle frequency response function. The surface frequency irregularity function in the frequency domain was used to determine the vertical and angular vehicle body transfer functions.

Siddharthan et. al. (2010) studied the field verification program details that were assumed to test the applicability of a finite layer mechanistic model chosen for calculating pavement responsiveness. The Fourier transform technique is used in this paper, which considers every pavement layer as continuous. As the tire imprint can vary in shape, this method can be used to analyze any type of tire imprint. Because the finite layer approach entails several phases, it is critical to validate its application for usage in pavement response calculations. Two well-documented full-scale field tests were used to validate the applicability of the proposed finite-layer technique and the computer application 3D – MOVE. The proposed finite layer approach is a powerful tool for simulating the visco-elastic behavior of asphalt concrete layers and evaluating the effects of vehicle speed and complex tire-pavement interface stresses on pavement responsiveness.

Kim et. al (2009) studied the effect of dynamic loads imposed on the pavement due to the moving vehicles have load magnitude variations due to the pavement roughness. The paper focused on the influence of the amplitude and wavelength on the surface roughness of the pavement due to the dynamic moving loads using artificial pavement profiles with triangular amplitude variation. Several different methods have been used to determine the pavement response when subjected to dynamic loads. After obtaining the pavement stresses, the AASHTO approach can be used to determine the pavement life. After the study was done, it was concluded that the dynamic loads become larger than the static loads with the increase in roughness of the surface. When the vehicle

speed is high, the dynamic loading magnitude is linearly proportional to the surface roughness amplitude and also increases dramatically with the static load.

Al-Qadi et. al. (2008) studied the vertical stress for the analysis over any other stresses or strain responses. The wave energy diminishes as it propagates through a pavement, and the lowest frequencies are the least damped. Because wave propagation is affected by the qualities of the pavement, the field pattern changes as the loading speed increases. The interaction of a moving vehicle with pavement roughness causes dynamic loading, and the frequency is governed by the roughness wavelength and vehicle speed. The vehicular load pulse was used to calculate the corresponding complex modulus at the dominant frequency. The results of this study demonstrated that if the loading frequency spectrum has enough energy to activate the natural frequency of the pavement, vibration can be felt after the loading impulse.

Mulungye et. al. (2006) analyzed the flexible pavement for the effects of tire pressure, wheel configuration, and axle load variations of a transportation truck. The modeling of the pavement was done as a two-dimensional four-layered stratum using the Ansys/ED software. The wheels' capability to produce rutting was compared using the Vertical Stress Influence (VSI). The strains resulted from the finite element model for the single axle were found to be 2.2 times larger than compared to the dual tandem pair per unit load in the longitudinal direction and 1.5 times in the transverse direction, according to the damage factors estimated. The size of the contact path and the tire vertical stiffness fluctuate when the inflation pressure of the tire changes.

Sukumaran (2004) used finite element analysis to investigate the failure mechanism in a pavement system under moving aircraft loads. To carry out the analysis, Abaqus had been used. A finite element mesh has been used for analysis. The pavement material was divided into three parts – asphalt mixture, granular materials, and cohesive soil. The asphalt mixture was modeled as elastic material; granular materials (base and subgrade layer) are modeled using the Mohr-Coulomb material model.

Hadi and Bodhinayake (2003) used the finite element method for the analysis of flexible pavement. The pavement structure is analyzed and simulated as a finite element model when subjected to cyclic loading based on field data. The analysis was carried out using the Abaqus finite element program. The layers of the pavement are

treated as a solid continuum in the finite element method. The deflection is identical for both static and cyclic loading when all of the pavement layers are considered linear elastic. When non-linear materials are present, the deflection increases. It was observed that when cyclic loading was simulated with non-linear pavement materials, the deflection at the top of the subgrade was larger than when static loading was used with either linear or non-linear pavement materials. The results showed that when non-linear materials are present, displacement under cyclic loading is close to measured field values.

Hardy and Cebon (1994) studied the influence of loading frequency and vehicle speed using a dynamic road response model with idealized loads. The development and usage of a dynamic road response model was the only approach to examine and include the effect of speed and frequency in road response computation. The frequency of applied dynamic loads was shown to be insensitive to the established dynamic pavement response model, but not to the vehicle speed. To investigate the dynamic reaction of the pavement to dynamic tire forces, the convolution theory was simplified. The dynamic loads were found to be similar to those found on ordinary trunk roads during the analysis.

Uddin et. al. (1994) carried out the parametric study using 3D finite element Abaqus software, which investigates the effects of pavement discontinuities and dynamic analysis on the surface deflection response of a pavement subgrade model. For a thorough pavement structural response analysis, finite element software such as Abaqus considers static and dynamic loads, linear elastic, and non-linear elastic models. The explicit and implicit techniques were used in the dynamic study on Abaqus. When comparing the two sets of findings, it was discovered that the deflection values obtained using the implicit method are closer to static deflections and higher than those acquired using the explicit method. A longitudinally cracked pavement's Abaqus dynamic maximum deflection is roughly 17% higher than an uncracked pavement's. A fractured pavement is expected to have higher dynamic deflections than an uncracked surface.

2.2 Research gap

In the previous studies, researchers studied either the velocity or frequency effect on the pavement. They research on-site and evaluated those results with numerical simulation. The researchers considered only one vehicle type for their study to see the effect of frequency or load on the pavement. However, there are very few studies where there has been numerical analysis done on different vehicle types. Also, numerical analysis considering different loads and vehicular frequency on a pavement profile is below par. The previously conducted studies focus on the effect of load and velocity of pavement deformation. And very few to no studies take into account the frequency effect on the pavement.

CHAPTER – 3

MATERIALS AND METHODOLOGY

3.1 Introduction to dynamic loads

The pavement dynamic response is highly influenced/affected by the speed of the vehicle and the roughness of the pavement. The service life of the pavement is considerably affected by the gross weight of the vehicle too. In the study, the vehicles are classified upon the use and then further classified according to gross vehicle weight (GVW) and axle configuration.

The evenness of the pavement is related to the vehicle movement dynamics. The moving loads from the vehicles vary from static to dynamic loads because of the roughness of the pavement. In comparison to the stresses caused by dynamic loads experienced by other structures, the stresses in the pavement structures are generally higher. Factors such as Dynamic Load Coefficient (DLC) and Dynamic Impact (DI) play an important role in determining the dynamic loading effect on the pavement. DLC is defined as the measurement of dynamic variation magnitude of the axle load for the specific combination of vehicle speed and pavement roughness. The values of DLC and DI are affected by the axle configuration, vehicle type, and speed, and lastly the pavement roughness or evenness (Dae-Wook Park, 2014).

The pavement roughness is calculated worldwide using the factor known as International Roughness Index (IRI). In India, the pavement roughness is calculated using Bump Integrator which tells about the pavement unevenness and is reported as Unevenness index (UI). From UI, the IRI is calculated as given by equation 3.1.

$$IRI = \frac{UI}{720} \quad \dots 3.1$$

3.2 Vehicle Classification

The vehicles are widely classified on the use, namely as commercial vehicles, and domestic vehicles. A commercial vehicle is defined as a vehicle that can transport goods and can carry 8 or more people. The gross vehicle weight defined for commercial vehicles is 4500 kg and above. These types of vehicles are generally owned by

organizations. A domestic vehicle is defined as a vehicle that is used for personal purposes. They can carry up to 6 or 8 people and the gross vehicle weight is limited to 1600 to 2000 kg.

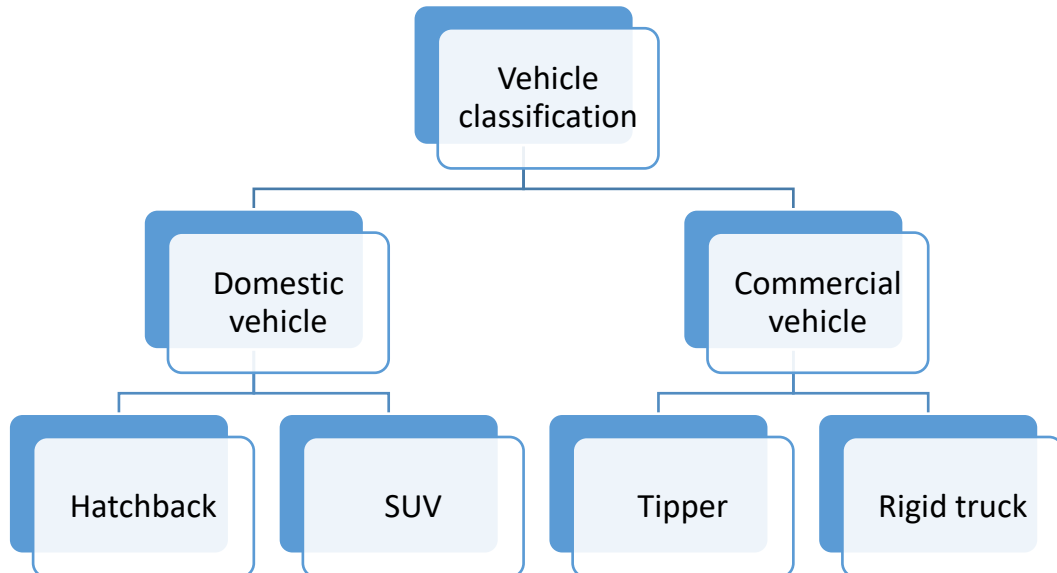


Figure 4 – Classification of vehicles

In this study, the vehicle data ranging from RPM, torque value, wheelbase radius, GVW has been taken from the respective company website. Each vehicle is classified as a domestic and commercial vehicle and further classified according to GVW, type (for commercial vehicle), and axle configuration (Table – 1 to 6).

Table 1 – Classification of domestic vehicle (Tata Motors 2021, Maruti Suzuki 2020, Hyundai 2021)

Company	Car name	Type
Tata	Tiago	Hatchback
	Nexon	SUV
Maruti Suzuki	Swift	Hatchback
	Vitara Breeza	SUV
Hyundai	Grand i10 Nios	Hatchback

Table 2 – Classification of commercial vehicles (Tata Motors 2021, Ashok Leyland 2021, Eicher 2018)

Company	Name	Type
Tata	Signa 1923.K	Tipper
	LPT 4225 Cowl & Signa 4225.T BS6	Rigid truck
Ashok Leyland	1920 TM	Tipper
	4225	Rigid truck
Eicher	Pro 6019T	Tipper
	Pro 6042	Rigid Truck

Table 3 – Types of commercial vehicles having GVW = 18500 kg and axle = 2 (Tata Motors 2021, Ashok Leyland 2021, Eicher 2018)

Name	Type	Axle	Torque @ RPM	Wheelbase (mm)
Tata Signa 1923.K	Tipper	2	850 Nm @ 1000 – 1600	3580
Ashok Leyland 1920 TM	Tipper	2	700 Nm @ 1200 – 2000	3600
Eicher Pro 6019T	Tipper	2	825 Nm @ 1200 – 1600	3635

Table 4 – Types of commercial vehicles having GVW = 42000 kg and axle = 5 (Tata Motors 2021, Ashok Leyland 2021, Eicher 2018)

Name	Type	Axle	Torque @ RPM	Wheelbase (mm)
Tata LPT 4225 & 4225.T BS6	Rigid Truck	5	950 Nm @ 1000 – 1800	6800
Ashok Leyland 4225	Rigid Truck	5	900 Nm @ 1200-2000	6600
Eicher Pro 6042	Rigid Truck	5	1000 Nm @ 1000 – 1700	6800

Table 5 – Classification of domestic vehicles having GVW = 1335 kg and axle = 2
(Tata Motors 2021, Maruti Suzuki 2020, Hyundai 2021)

Name	Torque @ RPM	GVW (kg)	Wheelbase (mm)	Axle
Maruti Suzuki Swift	113 Nm @ 4400	1335	2450	2
Tata Tiago	113 Nm @ 3300	1335	2400	2
Hyundai Grand i10 Nios	113 Nm @ 4000	1335	2450	2

Table 6 – Classification of domestic vehicles having GVW = 1600 to 1700 kg and
axle = 2 (Tata Motors 2021, Maruti Suzuki 2020, Hyundai 2021)

Name	Torque @ RPM	GVW (kg)	Wheelbase	Axle
Maruti Suzuki Vitara Breeza	138 Nm @ 4400 RPM	1600	2500 mm	2
Tata Nexon	170 Nm @ 1750 – 4000 RPM	1650	2498 mm	2

3.3 Pavement and material properties

The pavement taken for the study is flexible as shown in Figure – 5. It is a three-layered pavement, namely, bitumen layer, sub-base layer, and subgrade layer. The design and material properties have been taken following IRC 37 – 2018. The stress is transmitted to the subgrade layer by the application of load with depth.

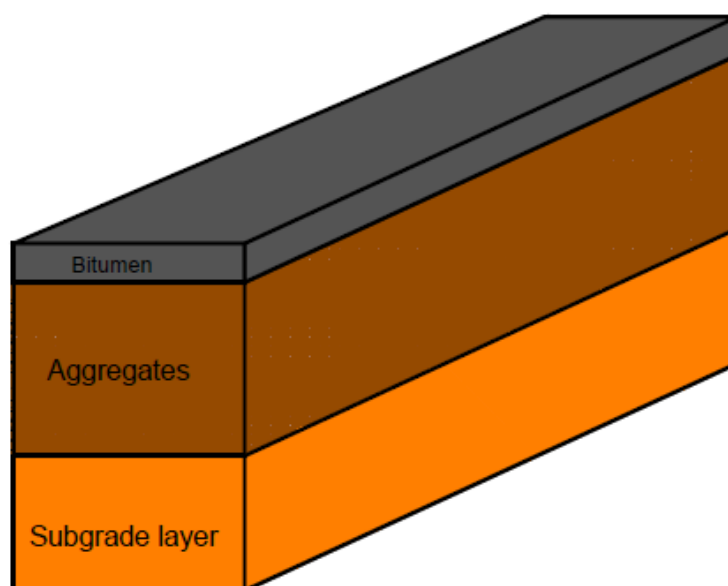


Figure 5 – A systematic model of flexible pavement layers used in modeling

The load on the flexible pavement gets transmitted through various layers. The load in the flexible pavement is distributed over a relatively smaller area of the subgrade beneath. The wheel stress is transferred from the top to bottom layer by grain-to-grain transfer through the contact points. The material properties such as young's modulus, Poisson's ratio, and density are given in Table - 7.

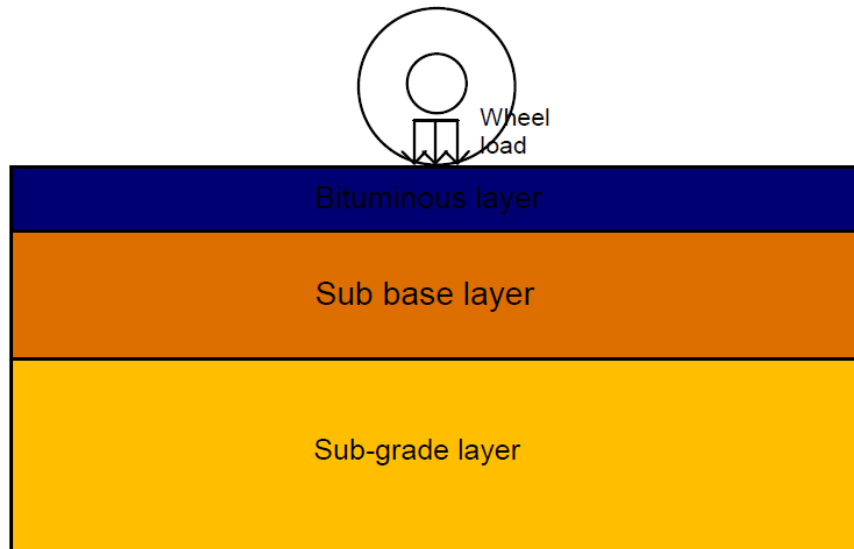


Figure 6 – Wheel load acting on the pavement

Table 7 – Material properties

Material	Young's modulus (MPa)	Poisson's ratio	Density (kN/m ³)
Bitumen	2 x 10 ⁶	0.25	10.29
Subgrade layer	2.76 x 10 ⁵	0.30	17.60
Sub-grade layer (soil)	5.15 x 10 ⁴	0.40	18.40

3.4 Dynamic formulae

In this study, the RPM value is taken as average and converted into frequency. The conversion formula is given by equation – 3.2.

$$1 \text{ RPM} = \frac{1}{60} \text{ Hz} = 0.016667 \text{ Hz} \quad \dots 3.2$$

The frequency response domain function represents the natural behavior of a vehicle (Barbosa. 1998). The irregularities that occur in the pavement are given by the spatial frequency (Barbosa, 2011). The relationship between time-frequency (ω), spatial frequency (n), and vehicle speed (V) is given by equation – 3.3 (Barbosa, 2011).

$$\omega = V \times n \quad \dots 3.3$$

where ω = frequency (Hz)

v = velocity of the vehicle (m/s)

$n = \frac{1}{\lambda}$ = inverse of the wavelength in meter

λ = wavelength (m)

Hence, the equation – 3.3 becomes

$$\omega = V \times \frac{1}{\lambda} \quad \dots 3.4$$

$$\lambda = \eta \frac{V}{\omega} \quad \dots 3.5$$

Table – 8 shows the wavelength of pavement roughness due to different velocities and frequencies from the vehicle. The value of η is taken as 0.9 which is a conversion factor. This helps to determine how the frequency and vehicle speed affect the pavement roughness.

Table 8 – Wavelength of pavement roughness due to various velocities of different vehicle types

Vehicle	RPM	Frequency (Hz)	Wavelength (mm) at different velocities		
			20 kmph	40 kmph	60 kmph
Tata Signa 1923.K	1300	21.67	25.631	51.274	76.911
Ashok Leyland 1920 TM	1600	26.67	20.830	41.661	62.492
Eicher Pro 6019T	1400	23.34	23.802	47.605	71.408
Tata LPT 4225 & 4225.T BS6	1400	23.34	23.802	47.605	71.408
Ashok Leyland 4225	1600	26.67	20.830	41.661	62.492
Eicher Pro 6042	1350	22.5	24.691	49.382	74.074
Maruti Suzuki Swift	4400	73.34	7.575	15.150	22.725
Tata Tiago	3300	55	10.101	20.202	30.303
Hyundai Grand i10 Nios	4000	66.67	8.332	16.665	24.998
Maruti Suzuki Vitara Breeza	4400	73.34	7.575	15.150	22.725
Tata Nexon	4000	66.67	8.332	16.665	24.998

From Table - 8, it is clear that as the velocity increases, at the same frequency, the wavelength of pavement roughness increases. And for the same speed, at different frequencies, the wavelength of pavement roughness decreases. The wavelength of pavement roughness has an inverse relationship with frequency at a particular velocity. On the other hand, at a particular frequency, the wavelength of pavement roughness and speed are directly proportional.

3.5 Application of soil dynamics

The nature of the dynamic loading on the structure depends on the source producing the dynamic loading (Das 1983; Ranjan and Rao 2018). The various studies that can be conducted using the soil dynamics application are –

- Earthquake study, vibrations produced in the ground, and propagation of waves through the soil
- Dynamic stress, deformation, and strength characteristics of the soil
- Dynamic earth pressure and bearing capacity problems
- Identification of settlement due to dynamic loading
- Solving problems related to liquefaction of soil
- Machine foundation design
- Designing of embedded foundation and piles under dynamic loading
- Embankment stability under dynamic loading

3.6 Finite Element Method

The numerical method to solve partial differential equations in 2 dimensions or 3-dimensional spaces is known as the finite element method. This method splits the larger system into smaller parts called finite elements. The study areas that include the finite element method are structural analysis, fluid dynamics, heat transfer, etc. (Gouri Dhatt, 2012). The division of the system into smaller parts has advantages such as –

- The complex geometry is represented accurately
- Different similar and dissimilar properties of materials can be put together
- Depiction of the solution easily
- Local effects captured

The basic idea or principle of the finite element method is the minimization of energy. In other words, when a specific boundary condition is given to a body, it can result in a variety of configurations, but only one is realistically achievable. The finite element method is consisted of using the unknown variables approximation to transform the partial differential equations into algebraic equations (Gouri Dhatt, 2012). The basic principles on which the finite element method is based are –

- i. To describe the partial differential equations, engineering sciences are used
- ii. For the elaboration and solution of algebraic equations, numerical methods are used
- iii. For carrying out the necessary calculations efficiently using a system, computing tools such as finite element method software is used

This study focuses on using the finite element method software, Abaqus to model and perform analysis of the flexible pavement. The version used for the study is Abaqus 2016 v6.14 by Dassault systems.

3.7 Steady-state dynamics analysis

The steady-state amplitude and phase of a system's response owing to harmonic excitation at a certain frequency are determined by steady-state dynamic analysis. Typically, such analysis is performed as a frequency sweep, in which the loading is applied at a succession of different frequencies and the response is recorded; with Abaqus/Standard, the frequency sweep is performed using the steady-state dynamic analysis process.

3.8 Assumptions

The key focus of this research work is to understand the effect of load and frequency of the vehicle on the flexible pavement using Abaqus. The software undertakes user-defined values and works on pre-defined assumptions. The following assumptions are made for carrying out the numerical analysis –

- The soil subgrade behavior is elastic in nature.
- The bitumen and subgrade layers are elastic in nature too.
- The analysis is done using a non-linear approach.
- The numerical model does not consider the damping coefficient.
- The friction between the surfaces is assumed to be 0.03

3.9 Modelling method

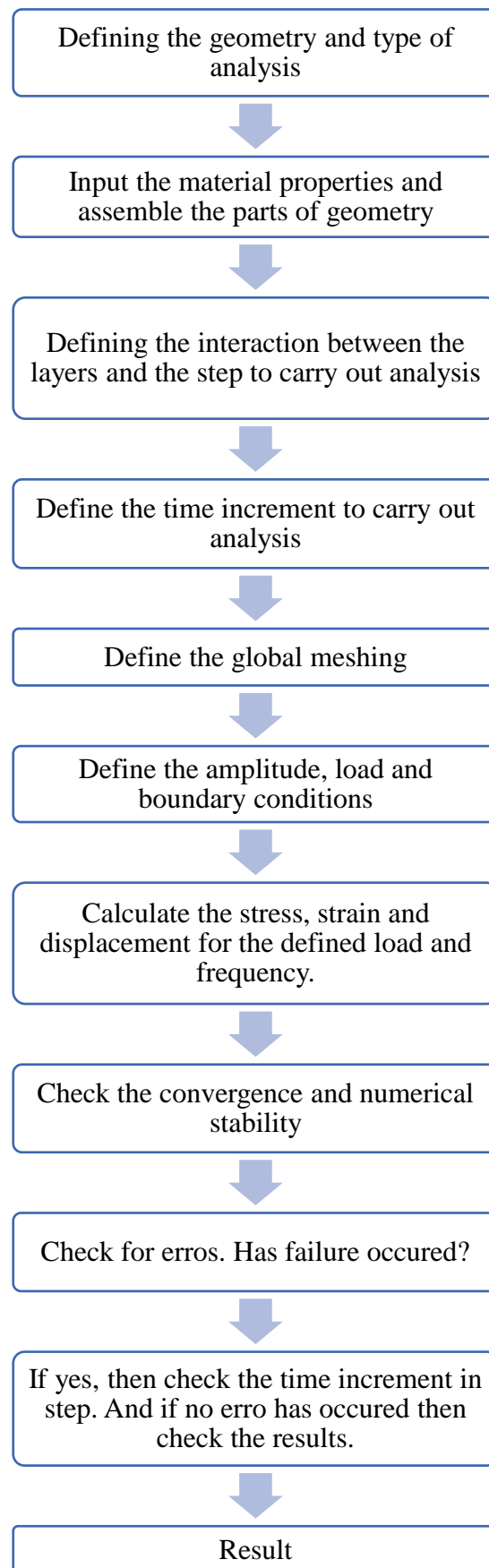


Figure 7 – Flow chart of the numerical analysis

The flowchart of the analysis carried out is shown in Figure – 7. The physical conditions of the system or structure are modeled as geometry and meshing is done accordingly. The limitations of the model are defined using the interaction property and boundary conditions. The model response to a load is known as the model behavior. The boundary conditions are necessary to define the problem area.

3.10 Model dimensions

As discussed in sub-topic – 3.3, the pavement is modeled as a three-layer flexible pavement having bitumen as the top layer, then subbase layer, and then the subgrade or subgrade layer (Figure – 8). The material properties are defined in Table - 7. The pavement dimensions modeled are given in Table – 9.

Table 9 – Pavement model dimensions

Layer	Length (m)	Width (m)	Height (m)
Bituminous surface	10	6	0.2
Subgrade layer	10	6	0.4
Subgrade layer	10	6	3

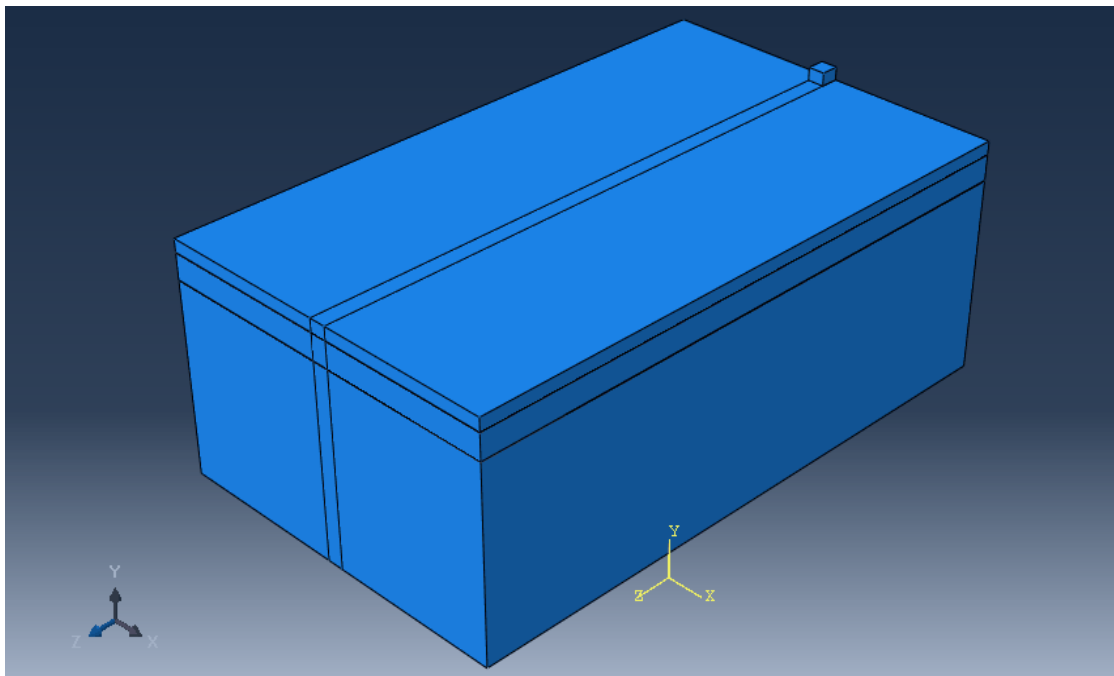


Figure 8 – Systematic view of flexible pavement modeled in ABAQUS

3.11 Meshing

The meshing helps to divide the larger parts into smaller nodes and subparts. To ensure that the results of the simulation/analysis are adequate and satisfactory, a properly refined and adequate mesh must be used. In analyses consisting of implicit or explicit approaches, coarse meshing produces inaccurate results. Finer the mesh, the more accurate the result. As the mesh density increases, the model numerical solution tends toward a unique solution. The meshing done is an 8-node brick element as shown in Figure – 9.

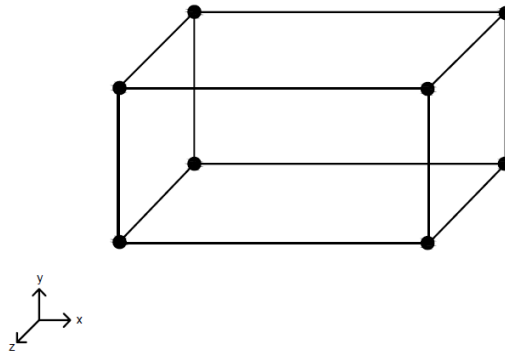


Figure 9 – 8 – Node brick element mesh

The meshing in the model is shown in Figure – 10. The meshing has been done fine to get accurate results. The size of the mesh element in the driving area is 0.20m X 0.28m. One must be well known to the mesh convergence condition in Abaqus explicit or implicit analysis. The model created is a solid continuum model. The meshing in the driving area is done finer than the whole assembly.

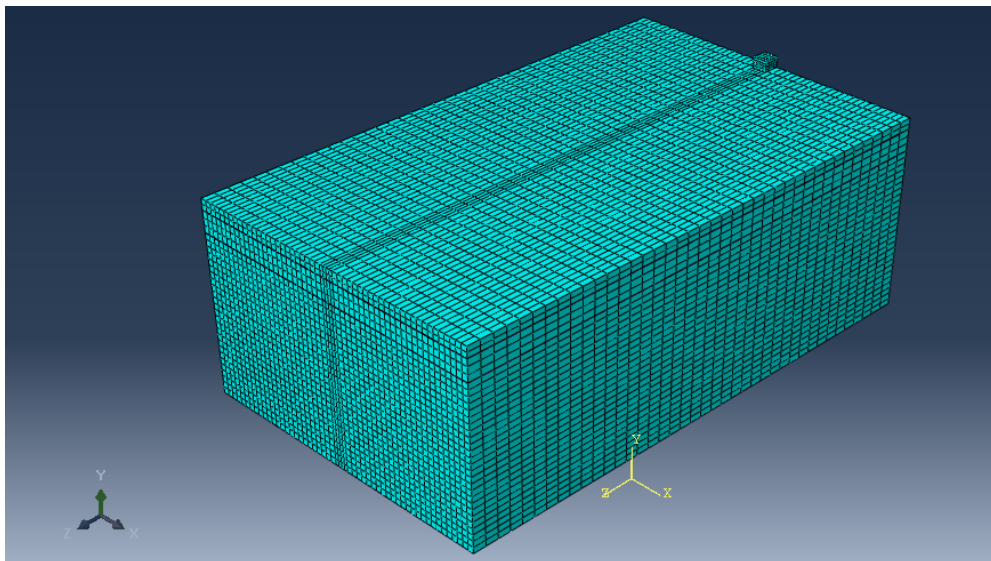


Figure 10 - Meshing in the model

3.12 Load and boundary condition

The interaction between the layers and the load surface is taken as general contact interaction. It means that the contact between the different layers of the model is within a single interaction. And the contact interaction property defines the tangential behavior, that is, friction and elastic slip, or the normal behavior of the model. The contact interaction property is defined under rigid contact or surface to surface contact.

3.12.1 Boundary conditions

The boundary condition used in the model is displacement/ rotation condition and encastre condition. This boundary condition is used to constraint the movement of the selected degree of freedoms in the model to zero or self-defined value.

3.12.2 Loads

As the analysis takes part in two steps, the first step is the application of load on the pavement and the second step is the vehicle moving step. The time increment taken is 0.01s in the vehicle moving step.

- The first step, that is, the load application step is the static analysis step, where the load is applied on the pavement.
- The second step, that is, the vehicle moving step is the dynamic analysis step, where the load applied in the first step moves according to the time increment specified over the surface.

The load is applied through a separate part which is static in the first step and moves in the second dynamic step. The load is applied through the bottom surface of the part on the pavement surface (Figure – 11). The different loads and amplitude are set which are given in Table – 11. The value of each amplitude is set according to a particular angular frequency given in Table – 10. The frequency obtained in Table – 8 is converted in angular frequency for the model by using equation 3.6.

$$\omega = 2\pi f \quad \dots 3.6$$

Where f = frequency (Hz)

ω = angular frequency (rad/s)

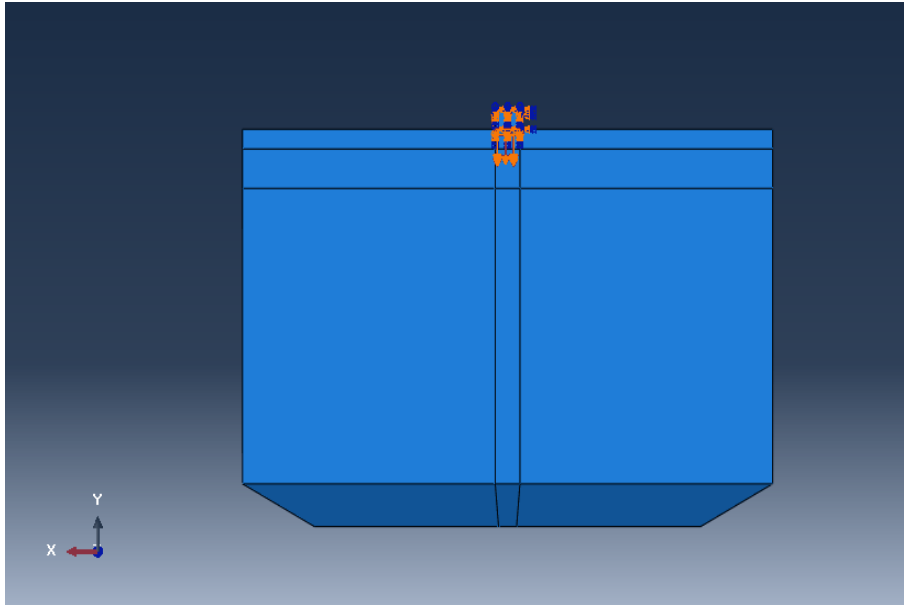


Figure 11 – Load application (shown by red downward arrows)

Table 10 – Value of load and amplitude used in the modeling

Load (in kg)	Frequency (Hz)	Angular frequency (rad/s)
18500	21.67	136.16
	26.67	167.57
	23.34	146.65
42000	23.34	146.65
	26.67	167.57
	22.5	141.37
1335	73.34	460.81
	55	345.58
	66.67	418.9
1600	73.34	460.81
	66.67	418.9

CHAPTER - 4

RESULTS AND DISCUSSION

4.1 Dynamic model validation

The most important aspect of any study is the evaluation of the numerical model results with the pre-existing condition. For the validation, the different material layers of the pavement structure were continuous, homogeneous, and isotropic in nature. It was assumed that there is no discontinuity between the layers and when the vertical load is applied, the layers don't move away from one another. The damping considered in the model is based on Rayleigh's damping criteria (Jianhong, 2020). The damping parameters are given in Table – 11.

Table 11 – Damping parameters (Jianhong, 2020)

Damping coefficient	5% (ζ)
α	2.6907
β	0.0009

Table 12 – Design parameters

Parameter	Bitumen		Subgrade		Subgrade	
	Jianhong (2020)	Present study	Jianhong (2020)	Present study	Jianhong (2020)	Present study
Young's modulus (MPa)	9000	2×10^6	300	2.76×10^5	80	5.15×10^4
Poisson's ratio	0.25	0.25	0.35	0.30	0.40	0.40
Density (kg/m ³)	2400	1049.29	2200	1794.60	1800	1876.28

The stress in the pavement structure is affected by the moving loads. To show the structural response due to the load at different locations, different nodes were created at different locations on the surface of every pavement layer. Three nodes were

created on the asphalt layer numbered 1, 2, and 3; three nodes numbered 4, 5, and 6 on the subgrade layer; three nodes numbered 7, 8, and 9 on the subgrade layer and three nodes numbered 10, 11, and 12 on the bottom surface of the pavement structure as shown in Figure – 23. The nodes 1, 4, 7, and 10 are situated at Point A distance from the origin, and the nodes 2, 5, 8, and 11 are situated at 3 m distance from the previous nodes and finally, the nodes 3, 6, 9, and 12 again at 3 m distance from the previous nodes (Figure – 12).

The pavement stress intensity is noted at these mentioned nodes. The analysis has been carried out using the Ansys software.

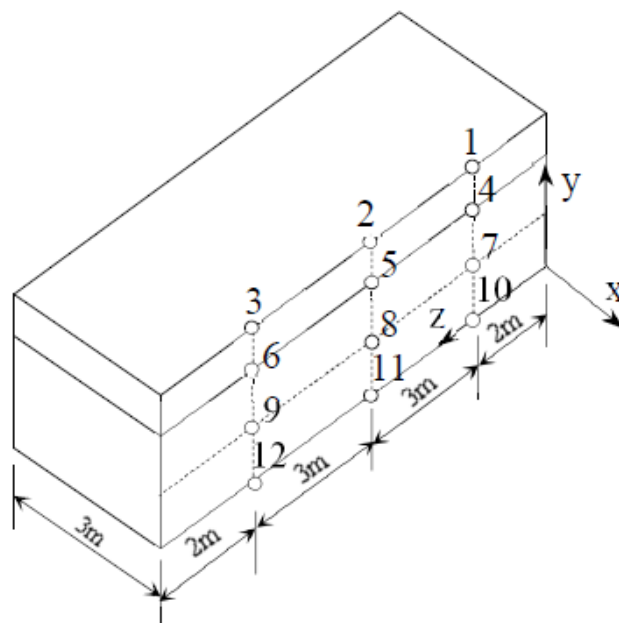


Figure 12 – Sectional view and nodes along the YZ plane (Jianhong, 2020)

The simulation for the validation model is done using the half-wave sinusoidal load with uniform moving speed given by equation – 4.1 (Jianhong, 2020).

$$P(t) = \left| P_m \times \sin\left(\frac{\pi}{T}t\right) \right| \quad \dots 4.1$$

$$T = \frac{12\delta}{V} \quad \dots 4.2$$

Where $P(t)$ = the distribution of load with time

t = time

P_m = load amplitude

T = load cycle

V = vehicle speed (m/s)

δ = tyre grounding area equivalent circle radius

The design parameters are $V = 12.5 \text{ m/s} = 45 \text{ kmph}$; axle load = 100 kN; $\delta = 0.1065 \text{ m}$ and $T = 0.10224 \text{ sec}$.

The peak stress obtained at each node is given in Table – 13. The results of the peak stress at different nodes from the study are compared with the simulation done on the Abaqus software which is given in Table – 13.

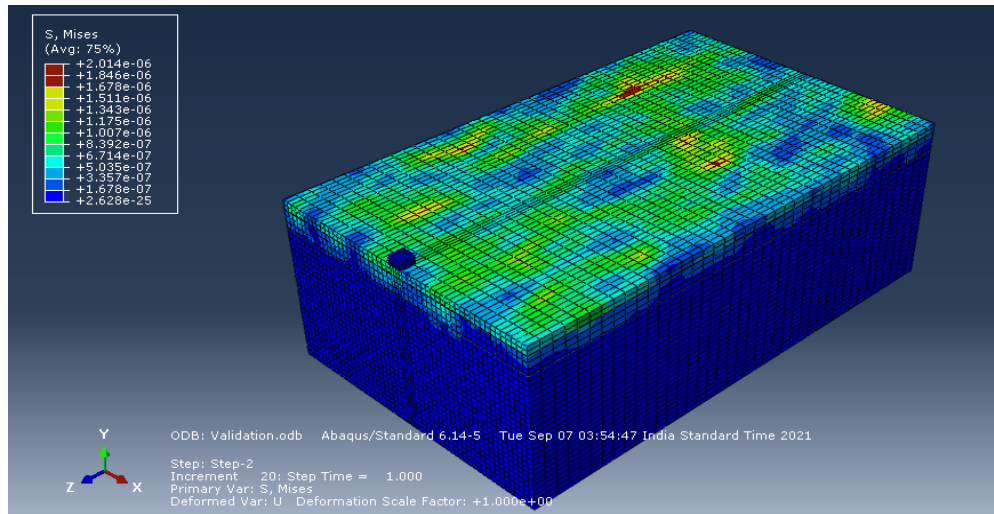


Figure 13 – Stress contour for the model at velocity 12.5 m/s

Table 13 – Stress intensity due to 100 kN load

Nodes No.	Stress intensity, kPa (Jianhong, 2020)	Stress intensity, kPa (Present study)
1	458.58	414.88
2	656.12	606.55
3	505.21	466.58
4	335.60	298.69
5	664.19	616.54
6	384.14	342.51
7	64.00	59.12
8	97.94	88.13
9	69.09	62.06
10	48.32	43.53
11	72.10	66.59
12	51.70	46.87

The results that are obtained using the Abaqus software show that the stress intensity value obtained is less than those obtained from Ansys software (Jianhong, 2020). The stress intensity values at the 12 nodes obtained from Abaqus software are 7 - 10% less than those obtained from the Ansys software. The error at every node is less than 20% which is desirable.

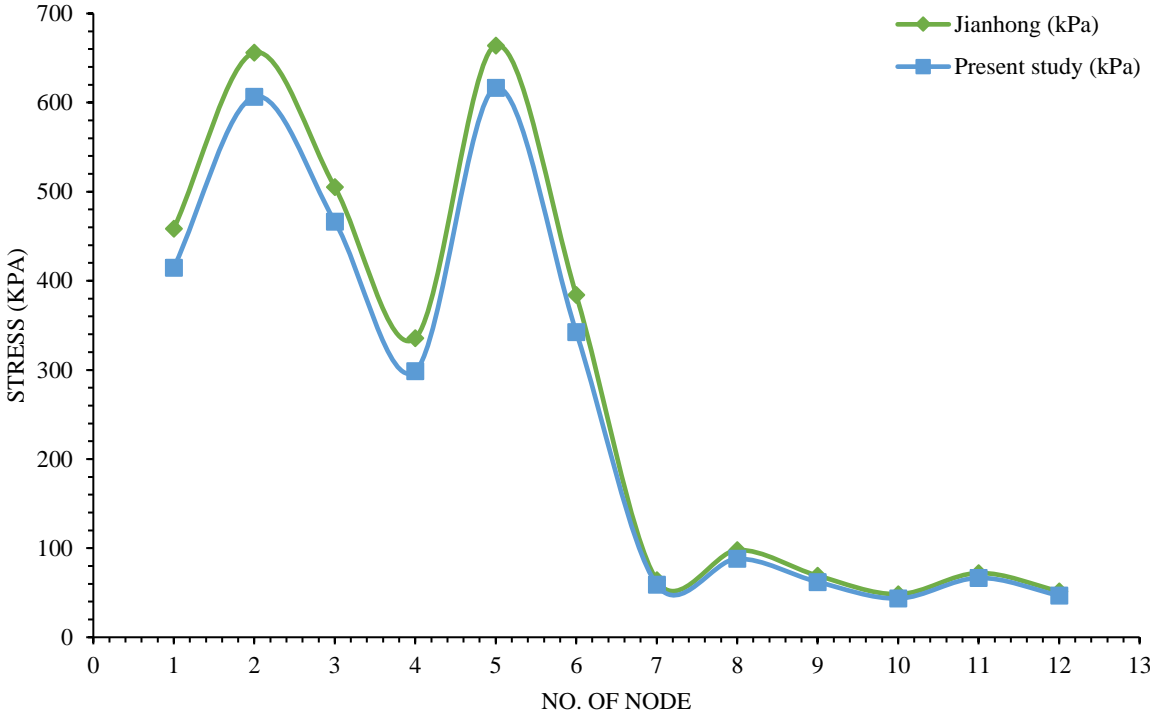


Figure 14 – Stress intensity at different nodes

4.2 Dynamic model analysis

4.2.1 Effect of speed on pavement stress intensity

Points A, B, and C are at 2 m, 5 m, and 8 m respectively from the initial position of the vehicle in the bitumen layer. Points D, E, and F are at 2 m, 5 m, and 8 m respectively from point of observation in the subbase layers. Similarly for the subgrade layer, points G, H, and I are at 2 m, 5 m, and 8 m respectively from the initial vehicle position.

4.2.1.1 When the speed of the vehicle is 20 kmph

When the vehicle moves at a speed of 20 kmph (5.55 m/s), the stress experienced by the different layers of the pavement is shown in Figure – 15. The stress variation at different points in different layers of the pavement is given in Figures – 16 to 18.

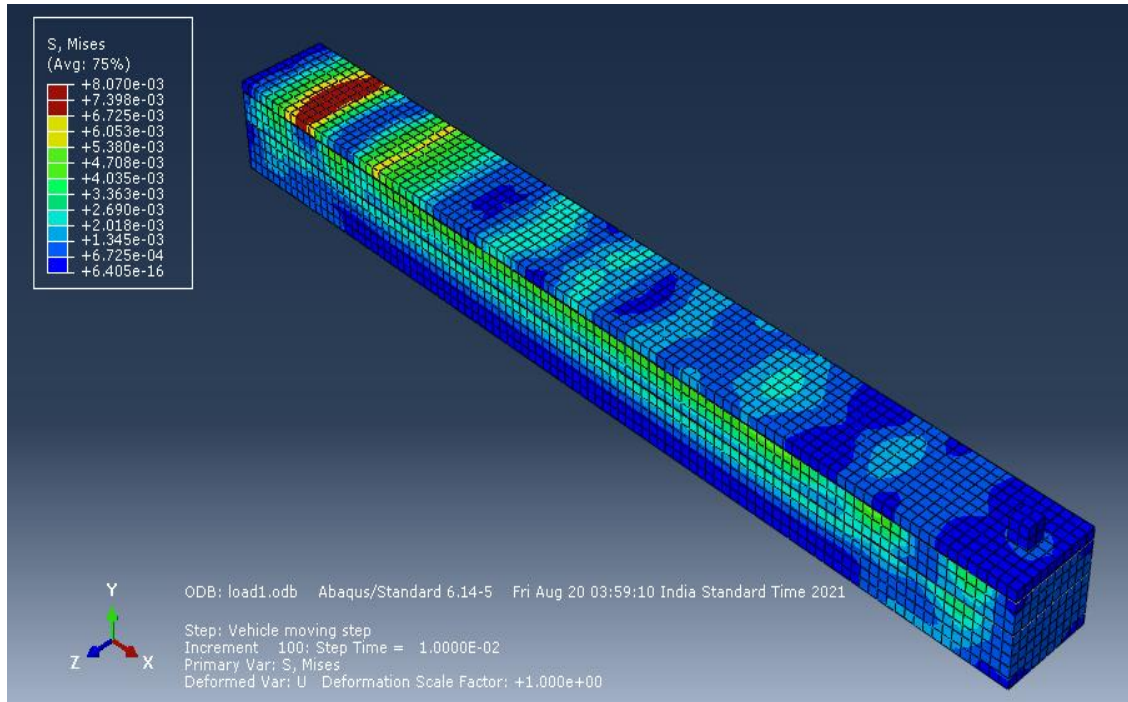


Figure 15 – Dynamic stress contour at velocity 5.55 m/s

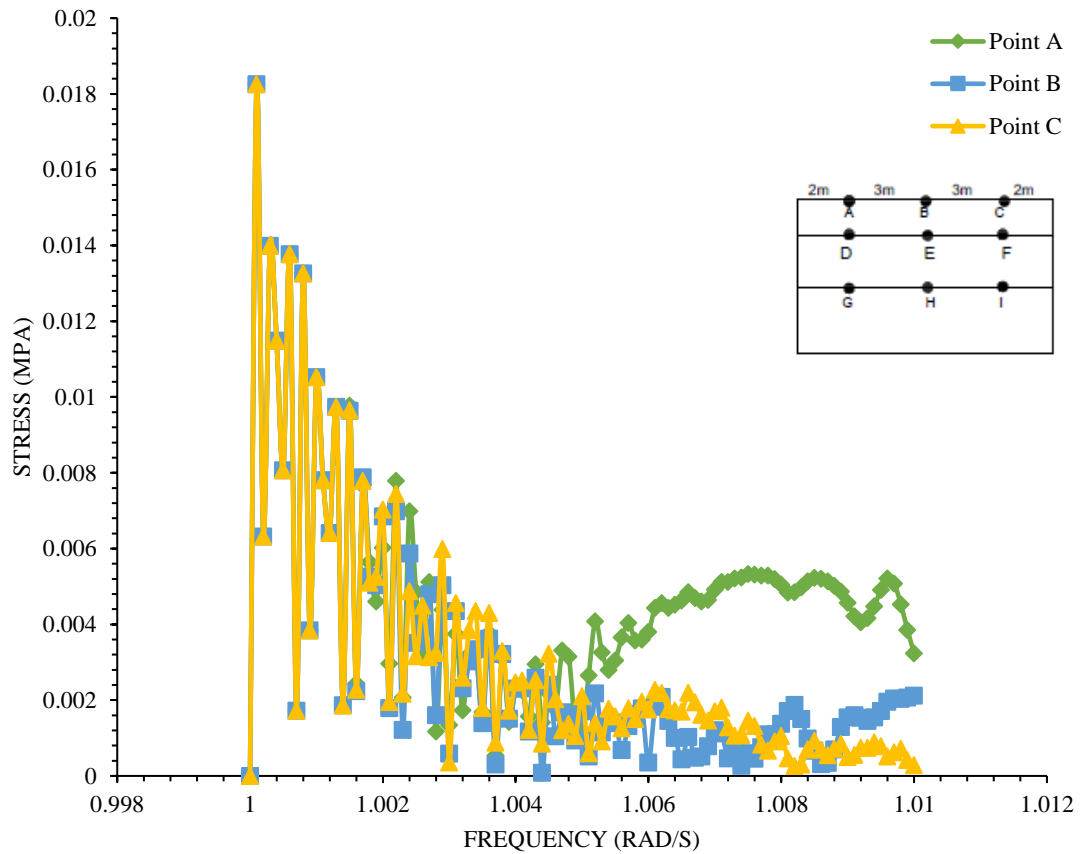


Figure 16 – Stress variation due to velocity 20 kmph in bitumen layer

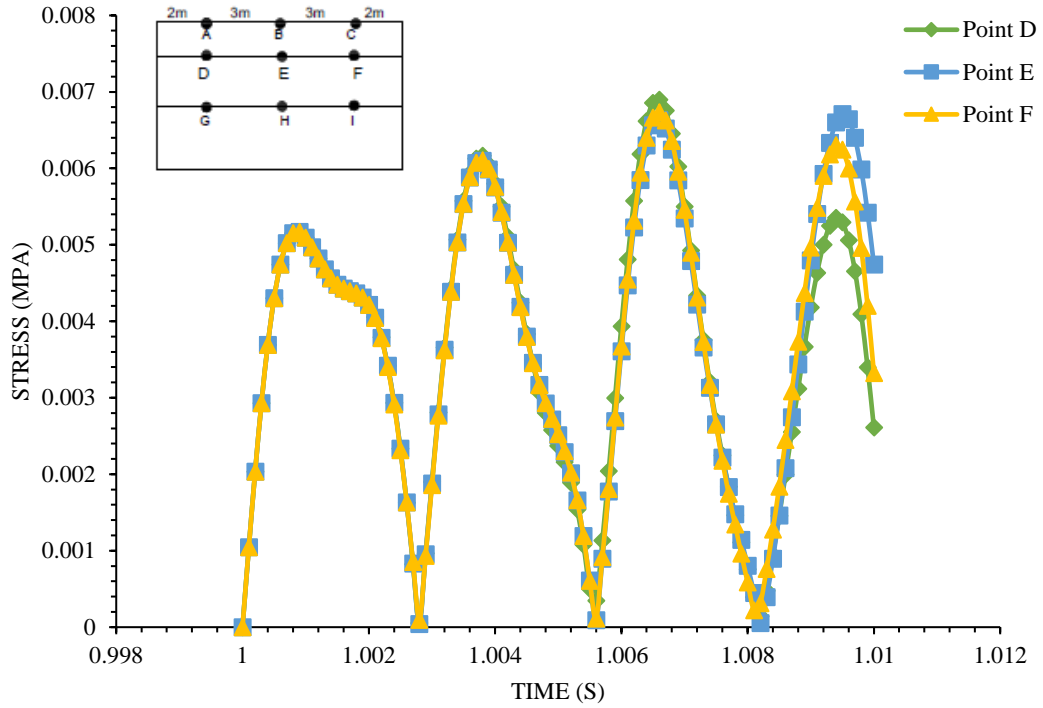


Figure 17 – Stress variation due to velocity of 20 kmph in the subbase layer

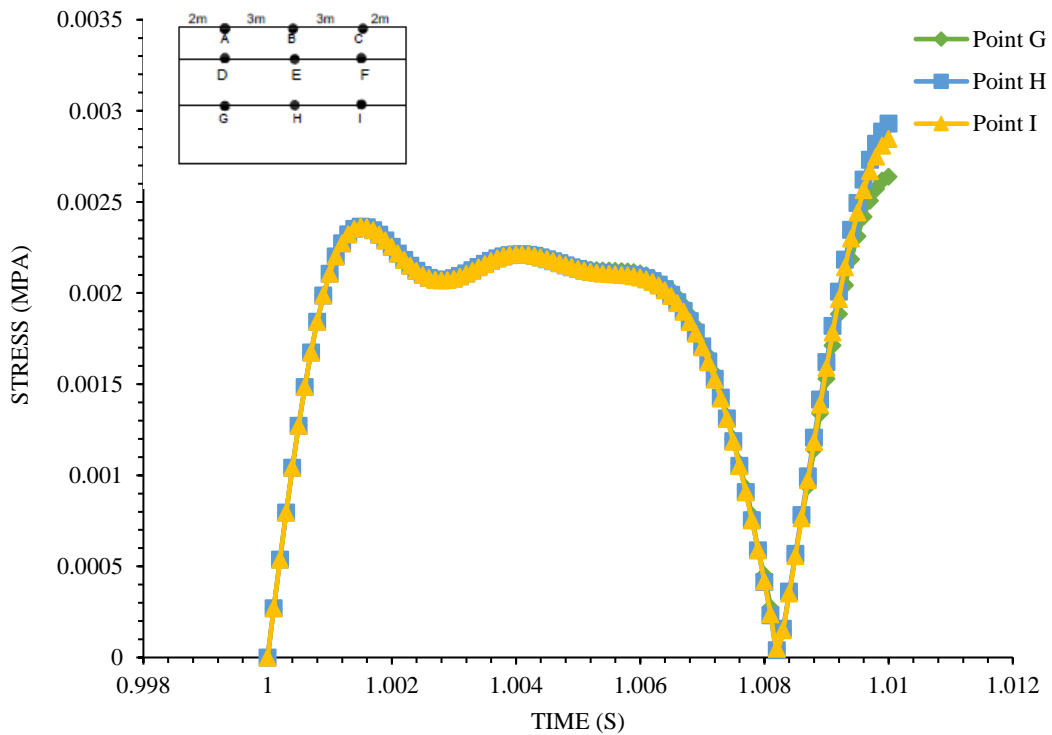


Figure 18 – Stress variation due to velocity 20 kmph in the subgrade layer

From Figure – 16, for the bitumen layer, the stress reaches its maximum value at the initial time and then decreases with an increase in time. At points A, B and C, the maximum stress value is 18.25 kPa or 0.01825 MPa obtained at time 1.0001s. In

comparison to Point B and C, the stress is more at Point A with an increase in time. The stress is minimum at Point C as the time increases. From Figure – 17, for a subbase layer, the maximum stress for Point D is 6.89 kPa or 0.00689 MPa obtained at time 1.0066s. The maximum stress for Point E is 6.70 kPa or 0.00670 MPa obtained at time 1.0066s. And for Point F, the maximum stress is 6.73 kPa or 0.00673 MPa obtained at time 1.0066s. From figure – 18, in the subgrade layer, the maximum stress at Point G is 2.63 kPa or 0.00263 MPa at time 1.001s. The maximum stress at Point H is 2.92 kPa or 0.00292 MPa obtained at time 1.0099s and the maximum stress at Point I is 2.84 kPa or 0.00284 MPa obtained at time 1.0099s. The stress decreases from bitumen to the subgrade layer.

4.2.1.2 When the speed of the vehicle is 40 kmph

When the vehicle moves at a speed of 40 kmph (11.11 m/s), the stress experienced by the different layers of the pavement is shown in Figure – 19. The stress variation at different points in different layers of the pavement is given in Figures – 20 to 22.

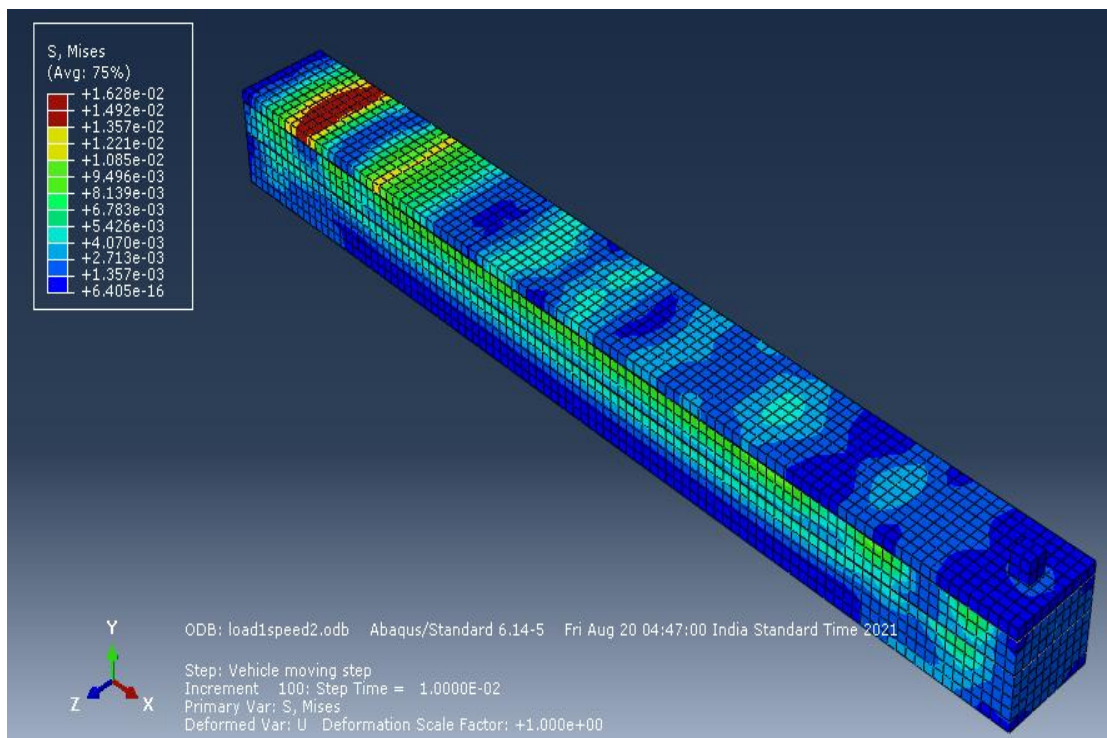


Figure 19 – Dynamic stress contour at velocity 11.11 m/s

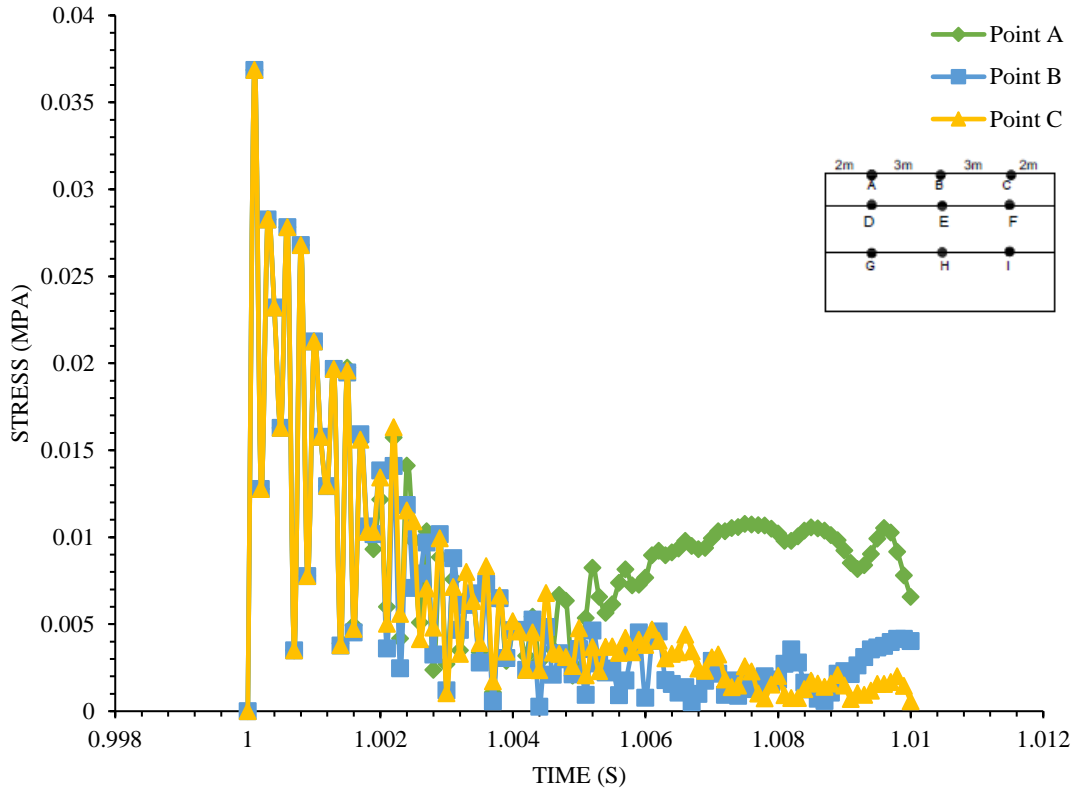


Figure 20 – Stress variation due to velocity 40 kmph in bitumen layer

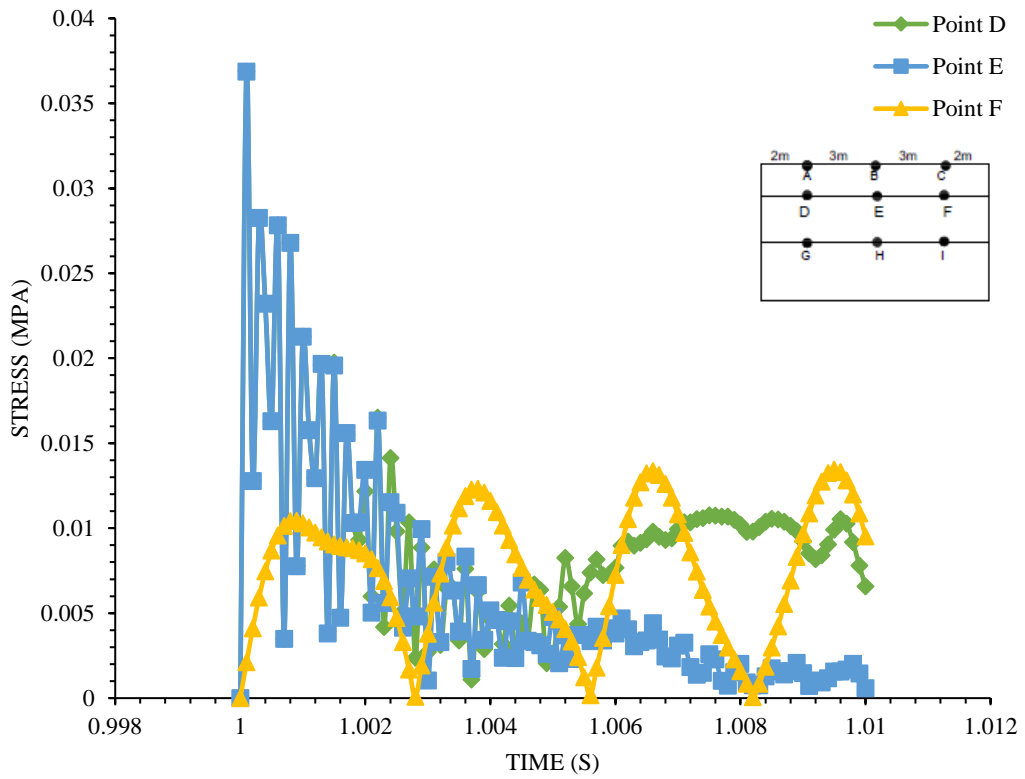


Figure 21 – Stress variation due to velocity of 40 kmph in the subbase layer

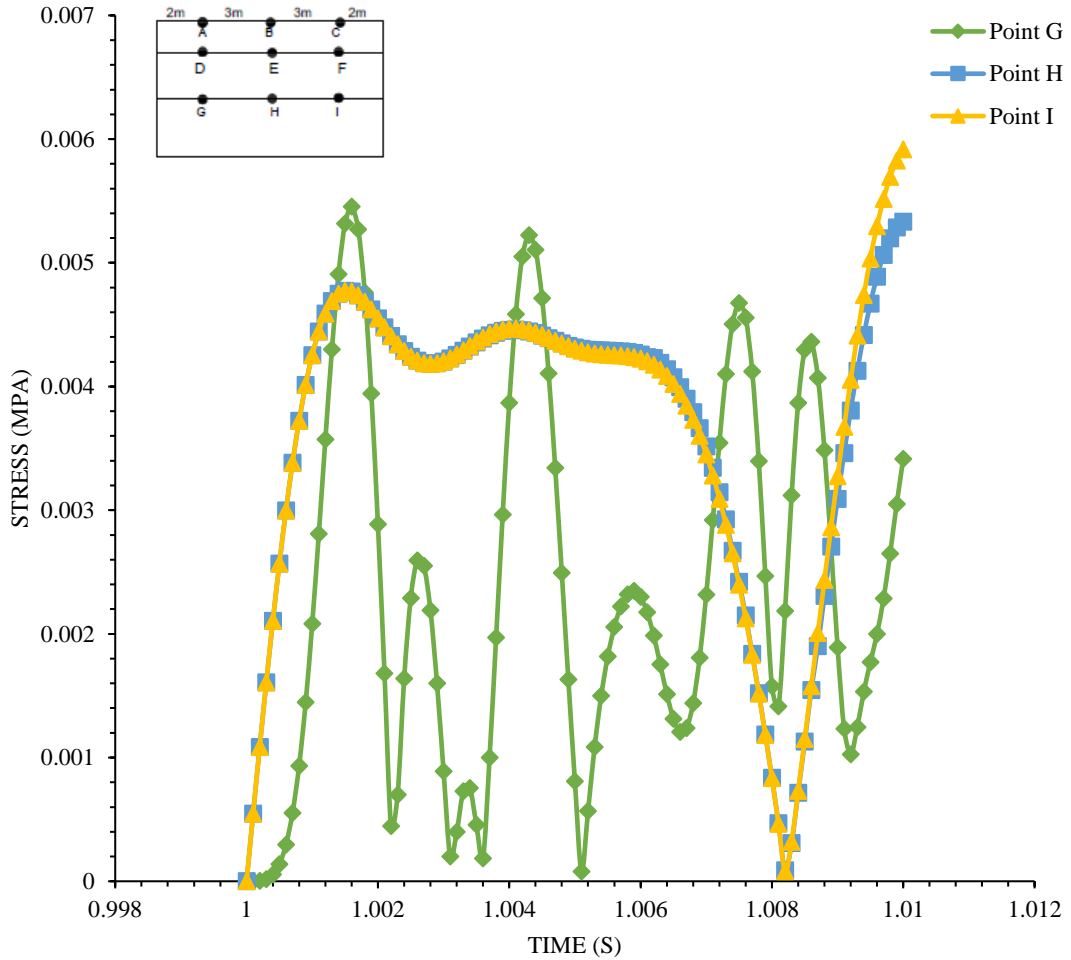


Figure 22 – Stress variation due to velocity 40 kmph in the subgrade layer

From Figure – 20, in the bitumen layer, the maximum stress obtained for Points A, B, and C is 36.87 kPa or 0.03687 MPa at time 1.001s. The maximum stress in the bitumen layer is obtained at the initial time. As the time increases, the stress decreases. At Point C, the stress is minimum than that at Point A and B. From Figure – 21, in the subbase layer, the maximum stress is the same for Point D and E, that is, 36.87 kPa or 0.03687 MPa obtained at time 1.0001s. This is the same as that obtained for the bitumen layer. The maximum stress at Point F in the subbase layer is 13.35 kPa or 0.01335 MPa obtained at time 1.006s. At Point F, the stress decreased in comparison to Point C. From Figure – 22, in the subgrade layer, the maximum stress for each point is different. The maximum stress at Point G is 5.45 kPa or 0.00545 MPa obtained at 1.0016s. For Point H, the maximum stress is 5.33 kPa or 0.00533 MPa obtained at 1.0099s. And the maximum stress at Point I is 5.91 kPa or 0.00591 MPa obtained at 1.0099s. The stress decreased from bitumen to the subgrade layer at each point.

4.2.1.3 When the speed of the vehicle is 60 kmph

When the vehicle moves at a speed of 60 kmph (16.67 m/s), the stress experienced by the different layers of the pavement is shown in Figure – 23. The stress variation at different points in different layers of the pavement is given in Figures – 24 to 26.

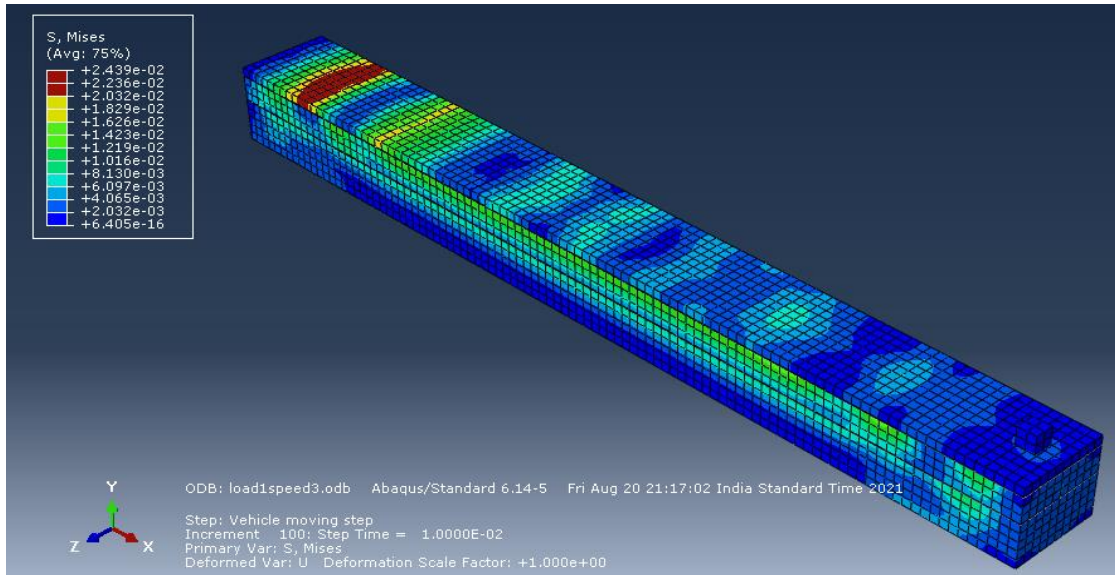


Figure 23 – Dynamic stress contour at velocity 16.67 m/s

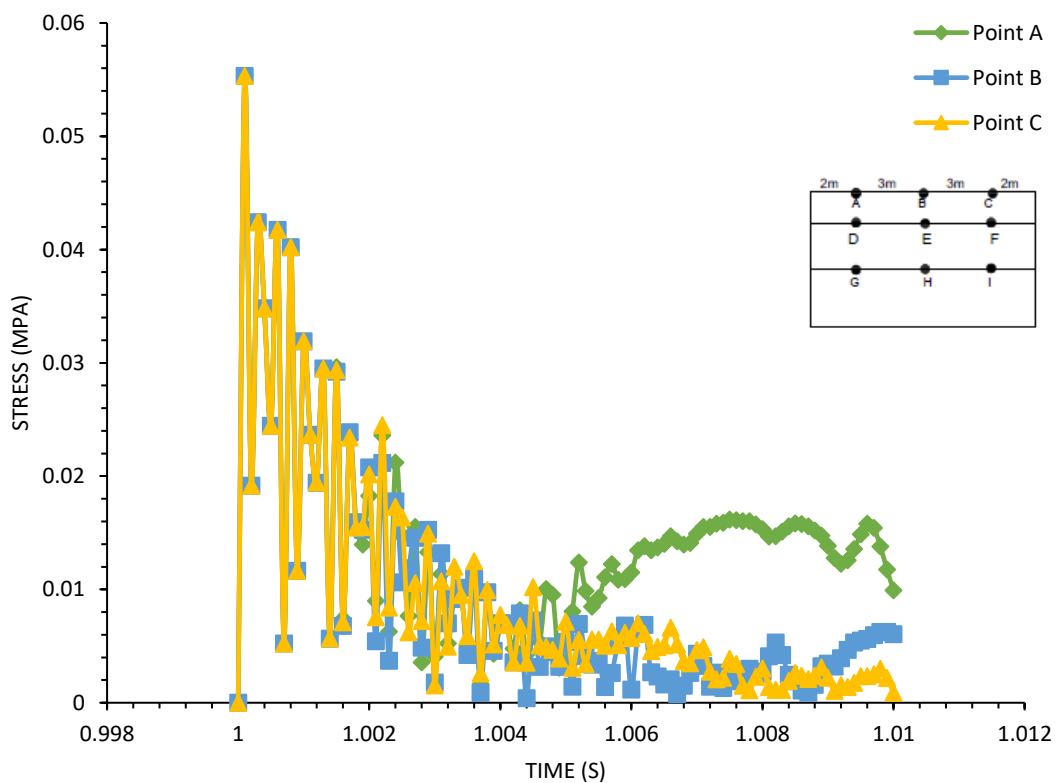


Figure 24 – Stress variation due to velocity 60 kmph in bitumen layer

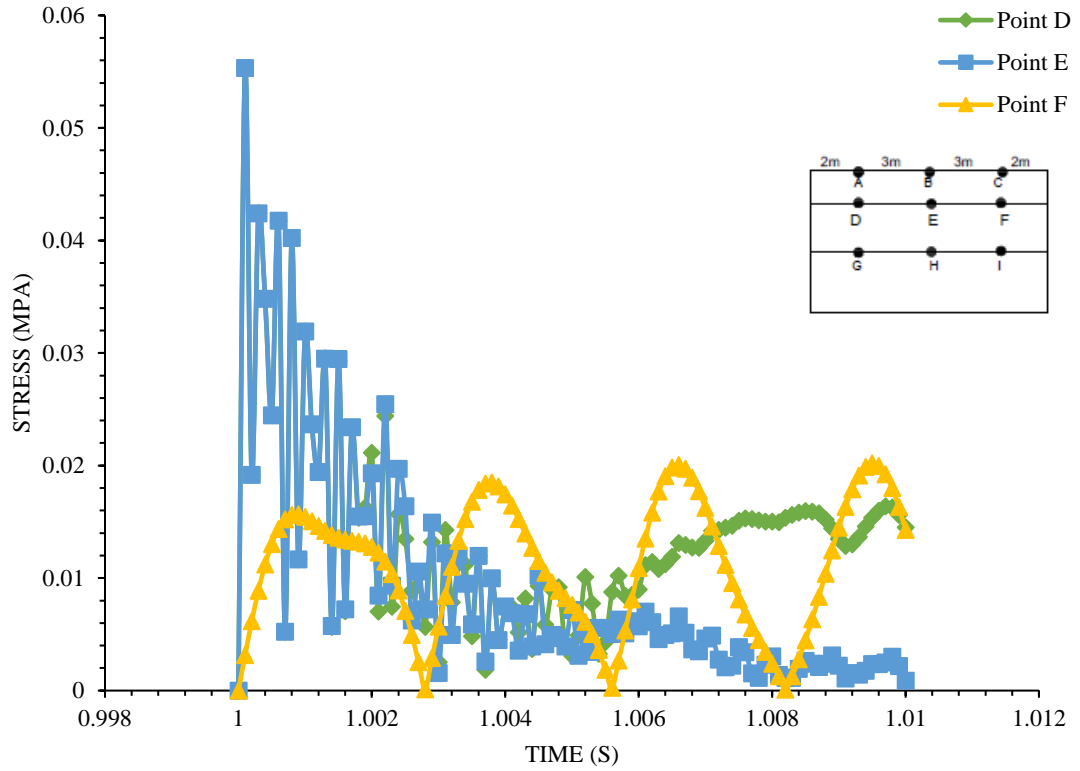


Figure 25 – Stress variation due to velocity of 60 kmph in the subbase layer

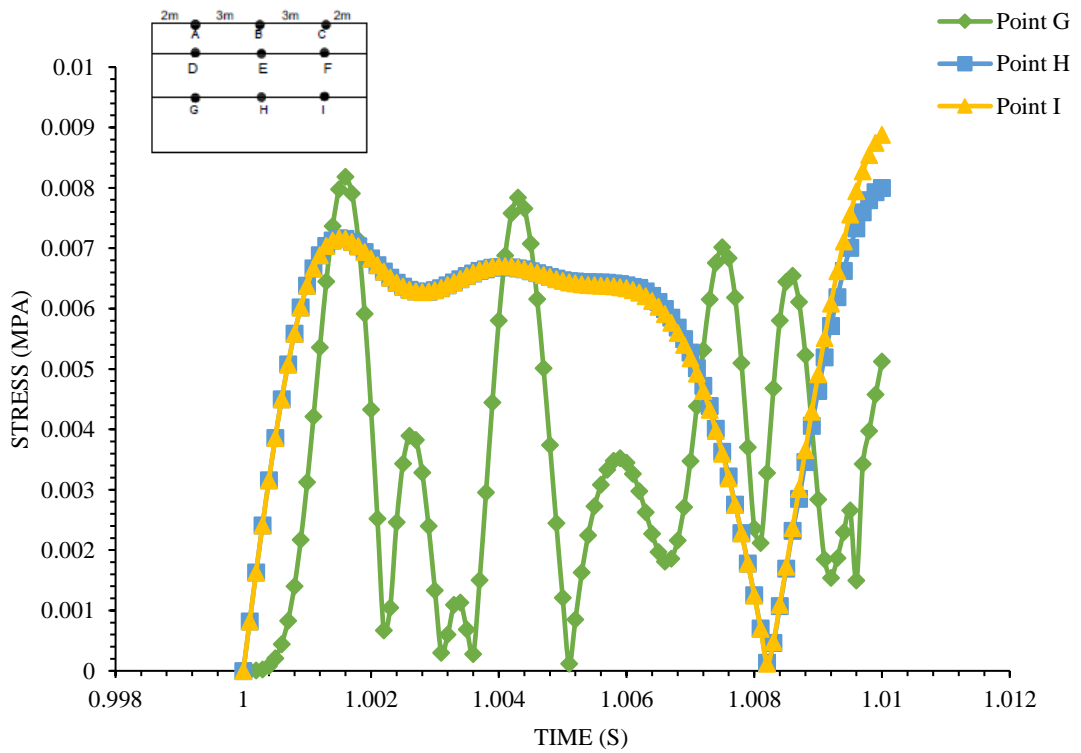


Figure 26 – Stress variation due to velocity 60 kmph in the subgrade layer

From Figure – 24, for the bitumen layer, the stress reaches its maximum value at the initial time and then decreases with an increase in time. At points A, B and C, the maximum stress value is 55.32 kPa or 0.05532 MPa obtained at time 1.0001s. In comparison to Point B and C, the stress is more at Point A with an increase in time. The stress is minimum at Point C as the time increases. From Figure – 25, for a subbase layer, the maximum stress for Point D and E is the same, that is, the stress is 55.32 kPa or 0.05532 MPa at time 1.0001s. And for Point F, the maximum stress is 19.95 kPa or 0.01995 MPa obtained at time 1.009s. From figure – 26, in the subgrade layer, the maximum stress at Point G is 8.18 kPa or 0.00818 MPa at time 1.0016s. The maximum stress at Point H is 7.99 kPa or 0.00799 MPa obtained at time 1.0099s and the maximum stress at Point I is 8.87 kPa or 0.00887 MPa obtained at time 1.0098s. The stress decreases from bitumen to the subgrade layer.

4.2.2 Maximum stress due to velocity

The present study includes 10 study points where the maximum stress is calculated at different velocities. Table – 14 shows the maximum stress values at different nodes and velocities.

Table 14 – Maximum stress at different velocities and nodes

Layer	Nodes	Maximum stress (kPa)		
		At 20 kmph	At 40 kmph	At 60 kmph
Bitumen	Point A (1)	18.25	36.87	55.32
	Point B (2)	18.25	36.87	55.32
	Point C (3)	18.25	36.87	55.32
Subbase	Point D (4)	6.89	36.87	55.32
	Point E (5)	6.7	36.87	55.32
	Point F (6)	6.73	13.35	19.95
Subgrade	Point G (7)	2.63	5.45	8.18
	Point H (8)	2.92	5.33	7.99
	Point I (9)	2.84	5.91	8.87

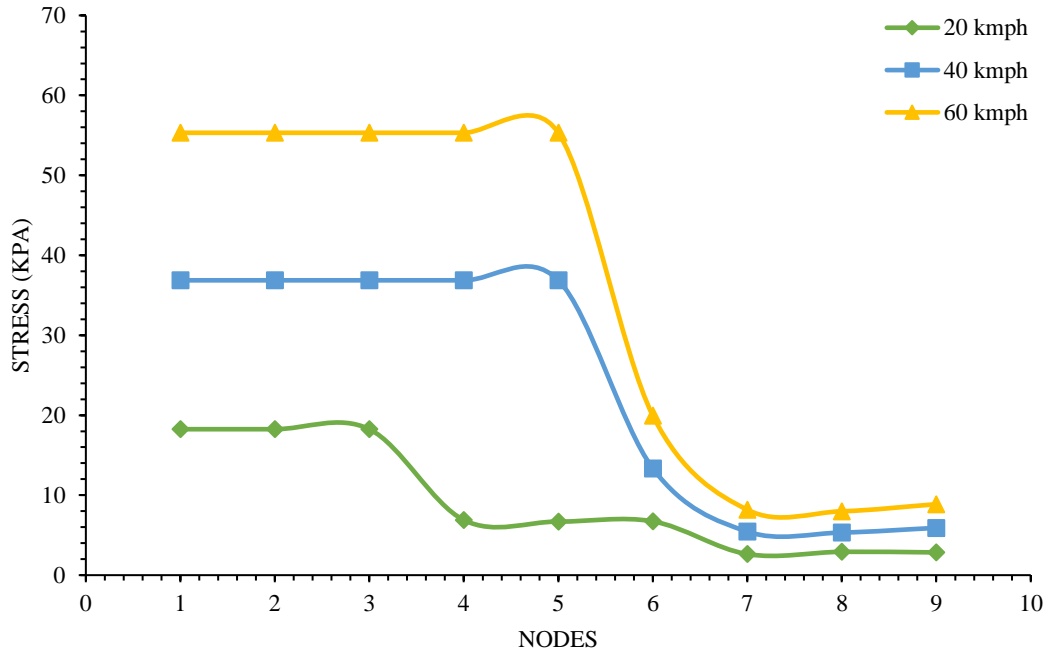


Figure 27 – Maximum stress at different nodes

From Figure – 27, it can be understood that the stress remains constant and then decreases. Also, the stress is more for higher velocity in comparison to lower velocity. For velocity of 20 kmph, the stress decreases from 18.25 kPa to 2.84 kPa and for velocity 40 kmph, the stress decreases from 36.87 kPa to 5.91 kPa and for 60 kmph, the stress decreases from 55.32 kPa to 8.87 kPa. As the velocity increased, the stress also increased from point to point, that is, from velocity 20 kmph to 40 kmph to 60 kmph, the stress increased from 18.25 kPa to 36.87 kPa to 55.32 kPa respectively. This shows that with an increase in velocity, the stress on the pavement also increases. The pavement stress and velocity have a direct relationship but as the vehicle moves along the pavement length, the stress and velocity have an inverse relationship.

4.2.3 Stress variation due to frequency in the pavement layers

4.2.3.1 Effect of frequency of vehicle having load 18500 kg (18.5 tonnes)

The frequencies taken for study under the vehicle load of 18.5 tonnes are 136.16 rad/s, 146.64 rad/s, and 167.57 rad/s. The displacement variation in the different layers, that is, in bitumen, subbase, and subgrade layer is given by Figure 28 – 30.

Table 15 – Stress variation due to the angular frequency for 18500 kg vehicle load

Layer	Angular Frequency (rad/s)	Point A (MPa)	Point B (MPa)	Point C (MPa)
Bitumen	136.16	200.73	209.37	256.56
	146.64	150.17	247.76	68.08
	167.57	55.72	82.83	33.82
Subbase	136.16	48.38	53.54	36.73
	146.64	123.02	138.60	106.61
	167.57	68.105	127.38	77.81
Subgrade	136.16	49.85	63.67	37.37
	146.64	89.53	98.25	71.34
	167.57	38.57	45.24	52.96

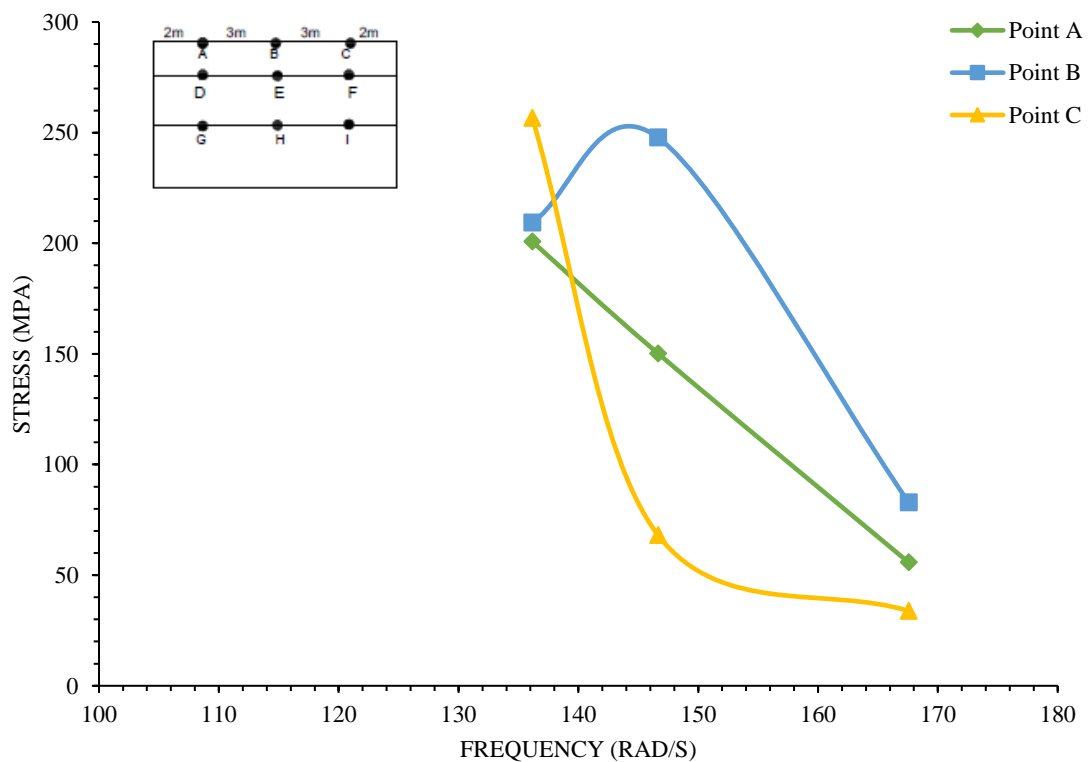


Figure 28 – Stress variation in bitumen layer for a vehicle load of 18500 kg

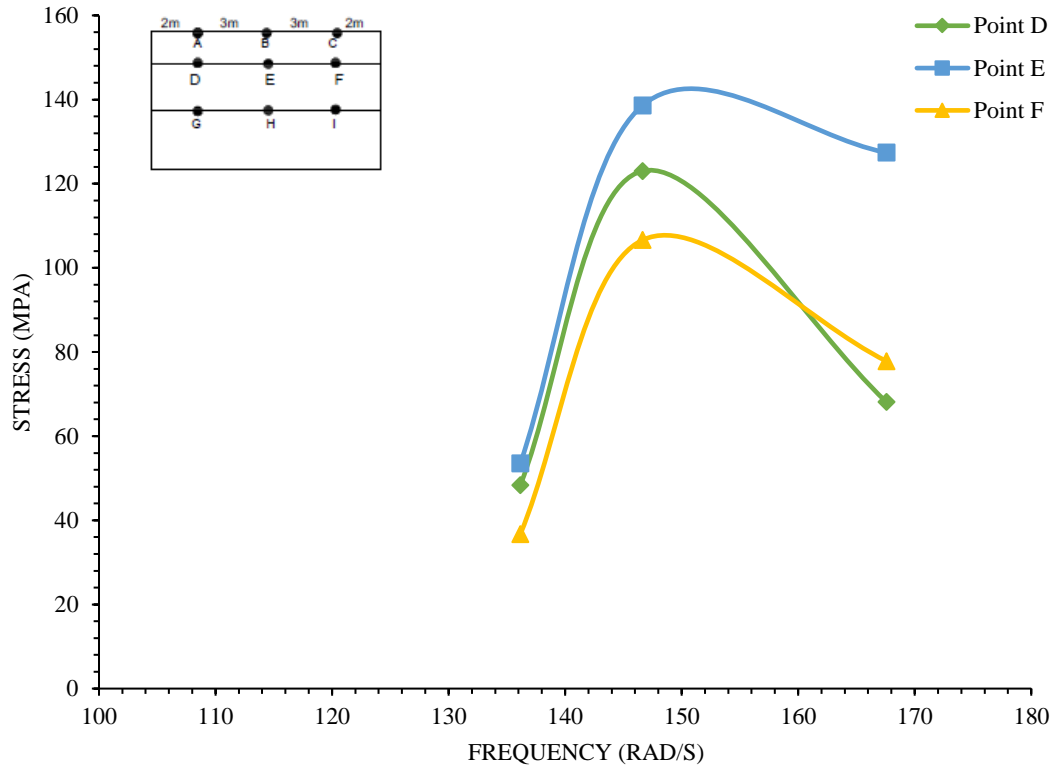


Figure 29 – Stress variation in the subbase layer for a vehicle load of 18500 kg

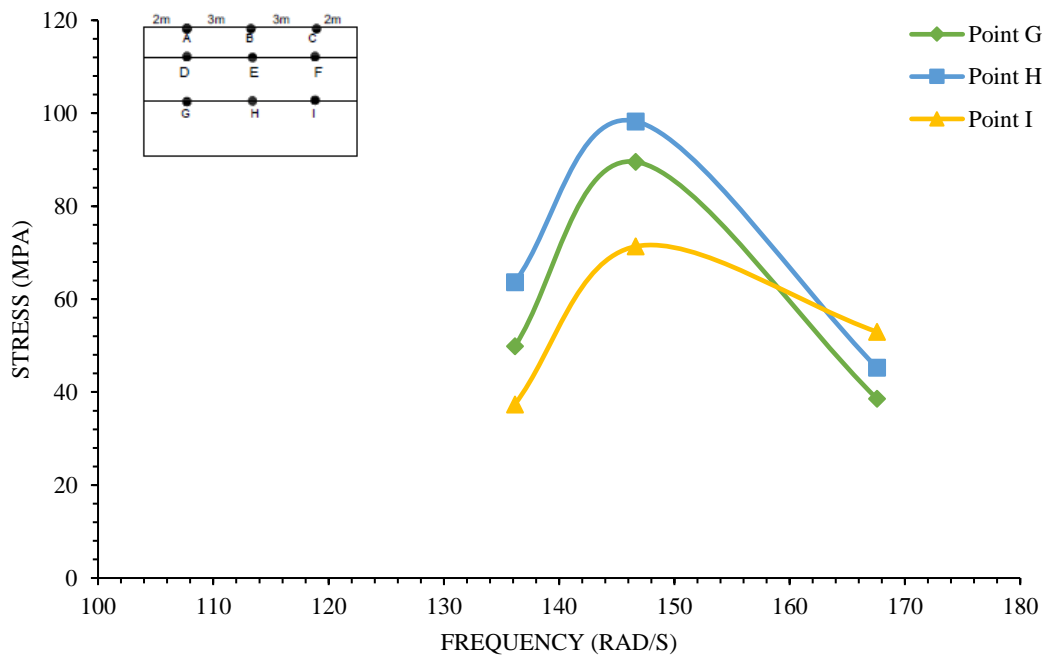


Figure 30 – Stress variation in subgrade layer for a vehicle load of 18500 kg

The stress variation in the three layers is different from each other. For the bitumen layer, the stress at Point A decreased with increasing frequency, that is, the stress for frequency 167.57 rad/s decreased to 55.72 MPa from 200.73 MPa at 136.16 rad/s

frequency. For the subbase layer, the stress increased from 48.38 MPa to 123.02 MPa but decreased to 68.105 MPa with an increase in frequency at Point D. For the subgrade layer, the stress variation at Point G was similar to that to the subbase layer at Point D. The difference in stress variation between the subbase layer and subgrade layer is that the stress is higher at frequency 167.57 rad/s than 136.16 rad/s for the subbase layer, whereas the stress is lower at frequency 167.57 rad/s for the subgrade layer. The stress variation at every point is that the stress increases from the initial point and then decreases except for the bitumen layer at frequency 136.16 rad/s. At this particular frequency in the bitumen layer, the stress increases from Point A to C which is not seen in any other layer and other frequency value.

4.2.3.2 Effect of frequency of vehicle having load 42000 kg (42 tonnes)

The frequencies taken for study under the vehicle load of 42000 kg are 141.36 rad/s, 146.64 rad/s, and 167.57 rad/s. The displacement variation in the different layers, that is, in bitumen, subbase, and subgrade layer is given by Figure 31 – 33.

Table 16 – Stress variation due to the angular frequency for 42000 kg vehicle load

Layer	Angular Frequency (rad/s)	Point A (MPa)	Point B (MPa)	Point C (MPa)
Bitumen	141.36	94.39	95.72	123.45
	146.64	195.43	202.56	149.40
	167.57	70.26	61.15	60.36
Subbase	141.36	70.38	62.13	22.25
	146.64	73.57	121.12	109.39
	167.57	62.49	61.05	40.44
Subgrade	141.36	31.84	37.02	40.69
	146.64	92.56	96.97	46.63
	167.57	29.83	31.49	47.99

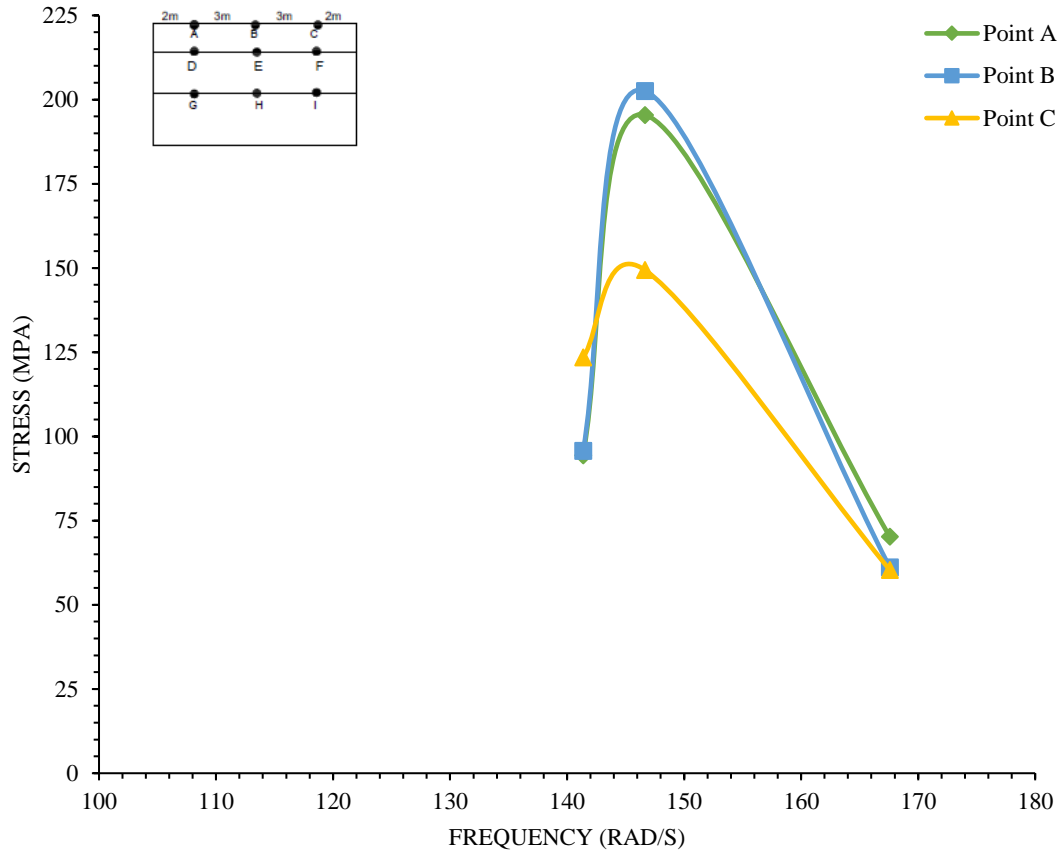


Figure 31 – Stress variation in bitumen layer for a vehicle load of 42000 kg

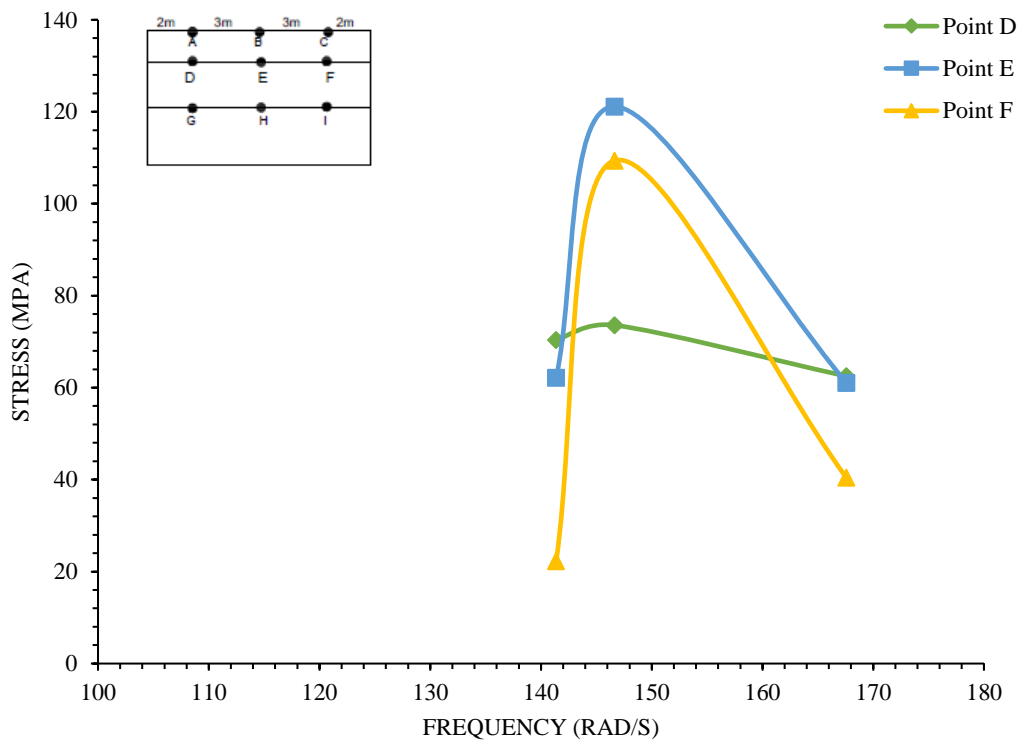


Figure 32 – Stress variation in the subbase layer for a vehicle load of 42000 kg

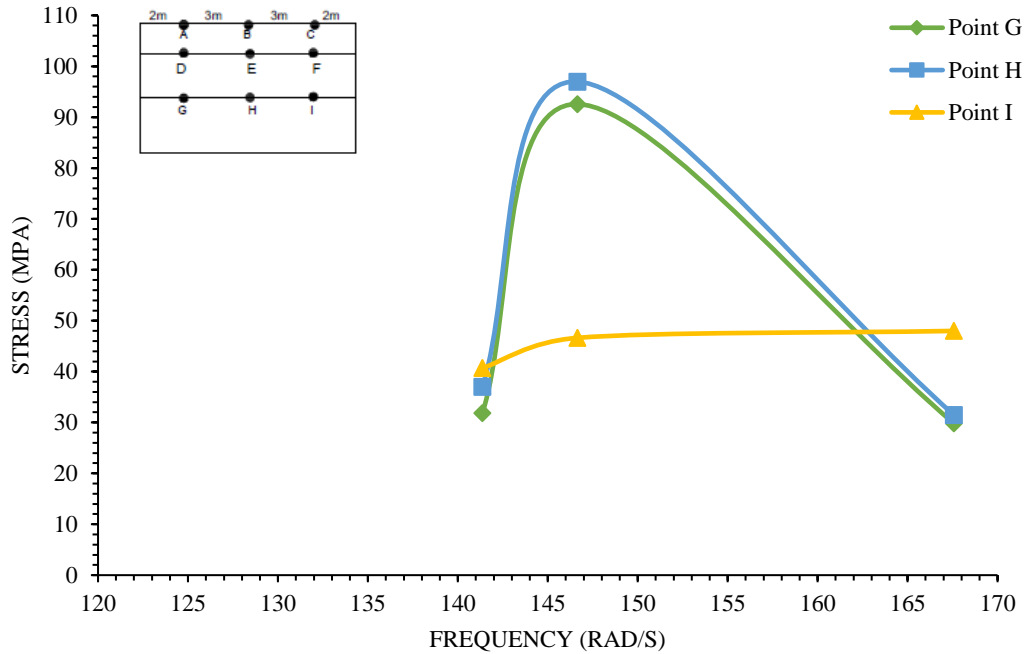


Figure 33 – Stress variation in subgrade layer for a vehicle load of 42000 kg

For the bitumen layer, at angular frequency 141.36 rad/s, the stress increases from Point A to C, that is, the frequency changes from 94.39 MPa to 123.45 MPa at the vehicle moves from Point A to C. But at angular frequency 146.64 rad/s, the stress increases from 195.43 MPa to 202.56 MPa at Point A to B but decreases to 149.40 MPa at Point C. And for angular frequency 167.57 rad/s, the stress decreases from 70.26 MPa to 61.15 MPa to 60.36 MPa at Point A to C. For the subbase layer, stress decreases from 70.38 MPa to 22.25 MPa at Point D to F for frequency 141.36 rad/s. For frequency of 146.64 rad/s, the stress increases from Point D to E and then decreases at Point F. And for angular frequency 167.57 rad/s, the stress decreases from Point D to F. The stress variation in the subgrade layer for angular frequency 141.36 rad/s and 167.57 rad/s is that the stress increases from Point G to I, that is, for frequency 141.36 rad/s the stress increases from 31.84 MPa at Point G to 40.69 MPa at Point I. And for frequency 167.57 rad/s, the stress increases from 29.83 MPa at Point G to 47.99 MPa at Point I. But for the frequency 146.64 rad/s, the frequency increases from 92.56 MPa at Point G to 96.97 MPa at Point H and then decreases to 46.63 MPa at Point I. The stress variation in all three layers is different from one another. Also, as the depth increases, the effect of frequency decreases, that is, from bitumen to subgrade layer, the stress decreases for any value of frequency.

4.2.3.3 Effect of frequency of vehicle having load 1335 kg (1.335 tonnes)

The angular frequencies taken for study under the vehicle load of 1335 kg are 345.57 rad/s, 418.59 rad/s, and 460.80 rad/s. The displacement variation in the different layers, that is, in bitumen, subbase, and subgrade layer is given by Figure 34 – 36.

Table 17 – Stress variation due to the angular frequency for 1335 kg vehicle load

Layer	Angular Frequency (rad/s)	Point A, D, and G (MPa)	Point B, E, and H (MPa)	Point C, F, and I (MPa)
Bitumen (Point A, B and C)	345.57	0.85	1.51	0.64
	418.89	1.09	2.69	1.52
	460.80	0.034	0.027	0.036
Subbase (Point D, E, and F)	345.57	0.512	0.741	0.575
	418.89	1.75	1.92	1.37
	460.80	0.042	0.054	0.040
Subgrade (Point G, H, and I)	345.57	0.336	0.309	0.504
	418.89	0.516	0.487	0.403
	460.80	0.011	0.017	0.013

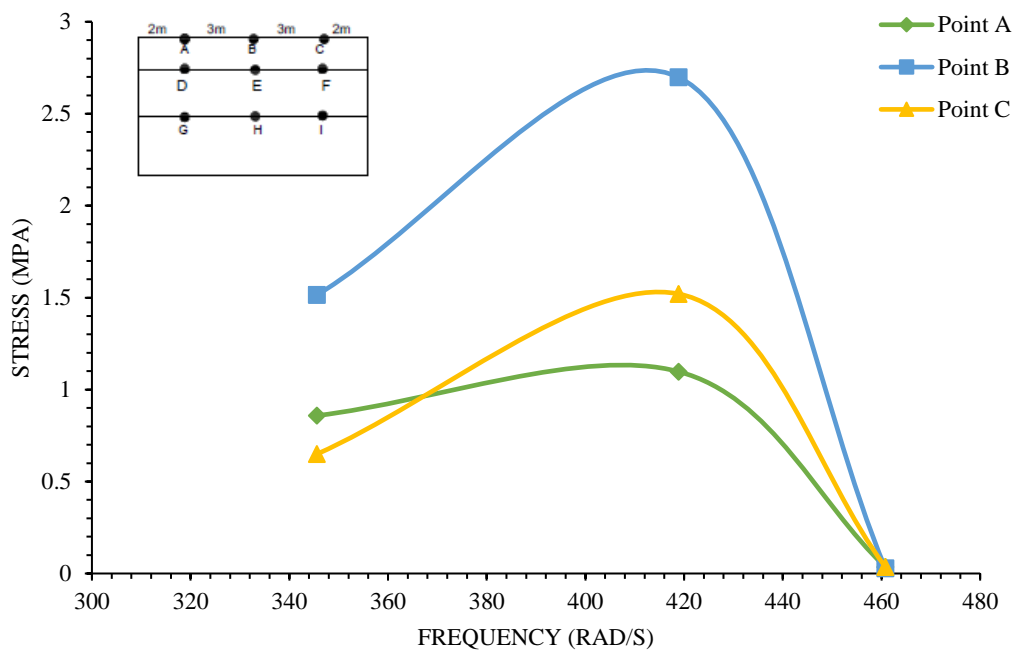


Figure 34 – Stress variation in bitumen layer for a vehicle load of 1335 kg

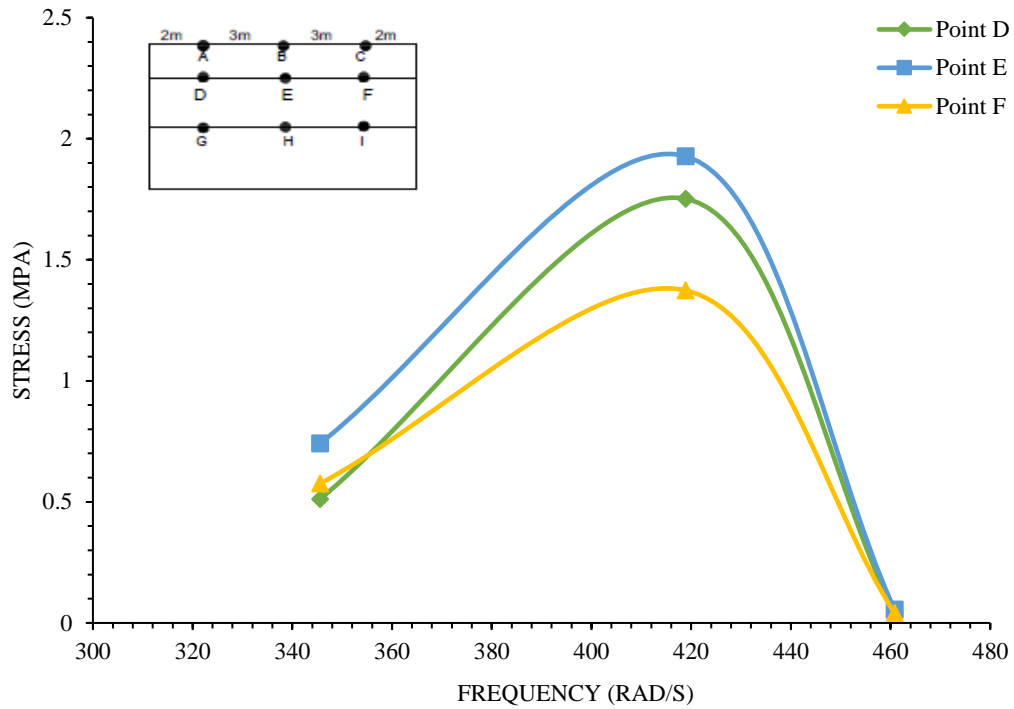


Figure 35 – Stress variation in the subbase layer for a vehicle load of 1335 kg

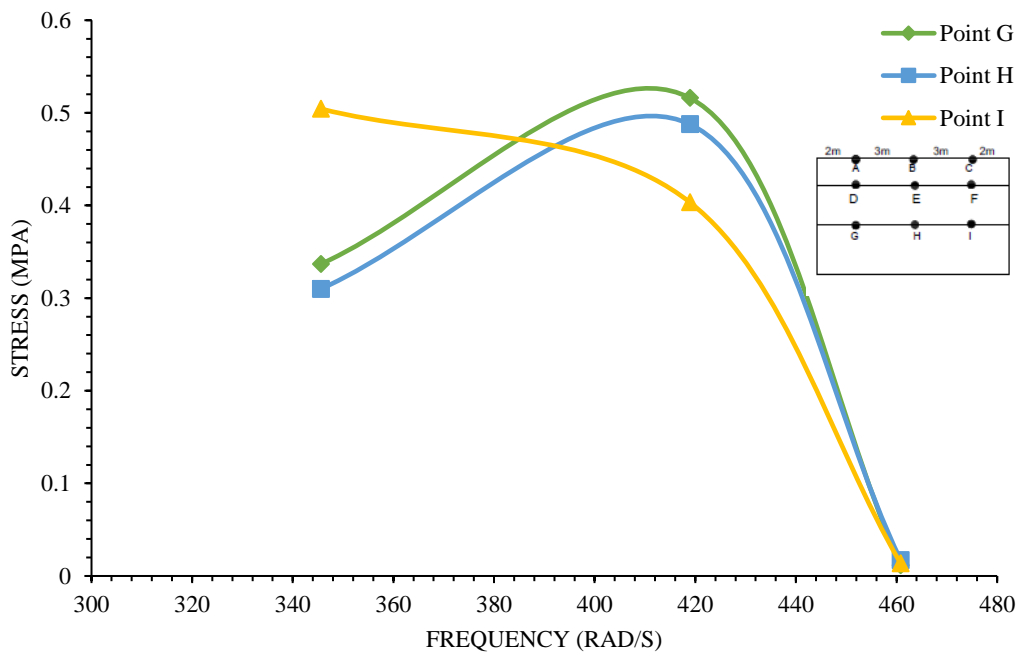


Figure 36 – Stress variation in subgrade layer for a vehicle load of 1335 kg

In the bitumen layer, for angular frequency 345.57 rad/s and 418.89 rad/s, the stress increases from Point A to B and then decreases at Point C. For angular frequency 345.57 rad/s, the stress increases from 0.85 MPa to 1.51 MPa at Point A to B and then decreases to 0.64 MPa at Point C. Similarly for angular frequency 418.89 rad/s, the stress changes from 1.09 MPa to 2.69 MPa to 1.52 MPa at Point

A to B to C respectively. But for frequency 460.80 rad/s, the stress decreases from 0.034 MPa at point A to 0.027 at Point B and then increases to 0.036 MPa at Point C. For the subbase layer, the stress variation for frequency 346.57 rad/s and 418.89 rad/s is the same as that in the bitumen layer. The stress increases from Point D to Point E and then decreases at Point F. But for frequency 460.80 rad/s, the stress variation in the subbase layer is different from the bitumen layer. At 460.80 rad/s, the stress increases from 0.042 MPa at Point D to 0.054 MPa at Point E and then decreases to 0.040 MPa at Point F. The stress variation in the subgrade layer is different for each frequency and varies from bitumen and subbase layer too. For frequency 345.57 rad/s, the stress decreases from 0.335 MPa at Point G to 0.309 MPa at Point H and increases to 0.504 MPa at Point I. For frequency 418.89 rad/s, the stress decreases from Point G to I. And for frequency 460.60 rad/s, the stress increases from 0.011 MPa at Point G to 0.017 MPa at Point H and then decreases to 0.013 MPa at Point I. But as the depth increases, that is, from bitumen to subgrade layer, the stress decreases for a particular frequency.

4.2.3.4 Effect of frequency of vehicle having load 1600 kg (1.6 tonnes)

The angular frequencies taken for study under the vehicle load of 1600 kg are 418.89 rad/s and 460.80 rad/s. The displacement variation in the different layers, that is, in bitumen, subbase, and subgrade layer is given by Figure 37 – 39.

Table 18 – Stress variation due to the angular frequency for 1600 kg vehicle load

Layer	Angular Frequency (rad/s)	Point A, D, and G (MPa)	Point B, E, and H (MPa)	Point C, F, and I (MPa)
Bitumen (Point A, B and C)	418.89	1.31	3.23	1.82
	460.80	0.041	0.032	0.043
Subbase (Point D, E, and F)	418.89	2.09	2.30	1.64
	460.80	0.050	0.065	0.048
Subgrade (Point G, H, and I)	418.89	0.618	0.584	0.483
	460.80	0.014	0.020	0.016

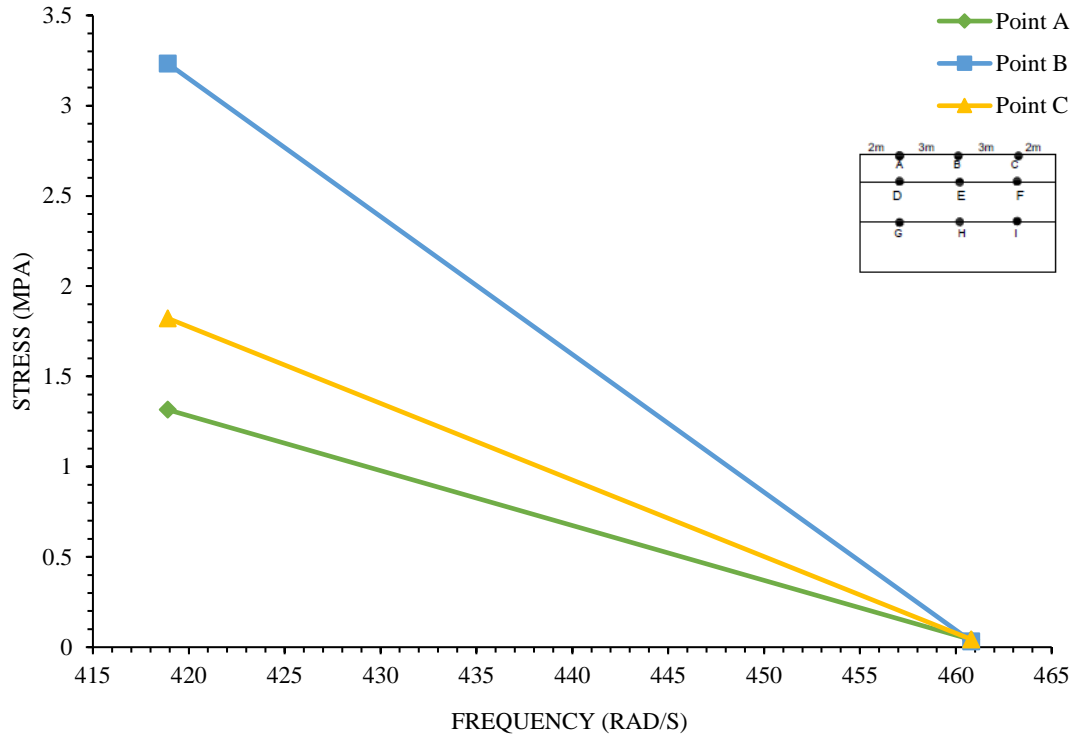


Figure 37 – Stress variation in bitumen layer for a vehicle load of 1600 kg

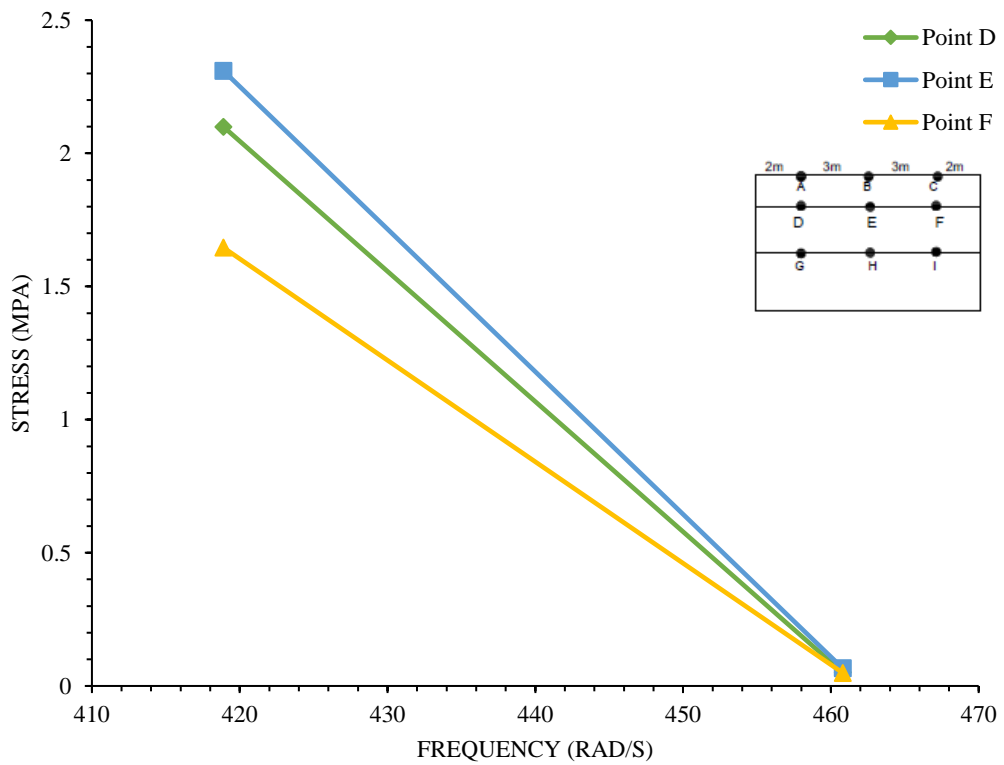


Figure 38 – Stress variation in the subbase layer for a vehicle load of 1600 kg

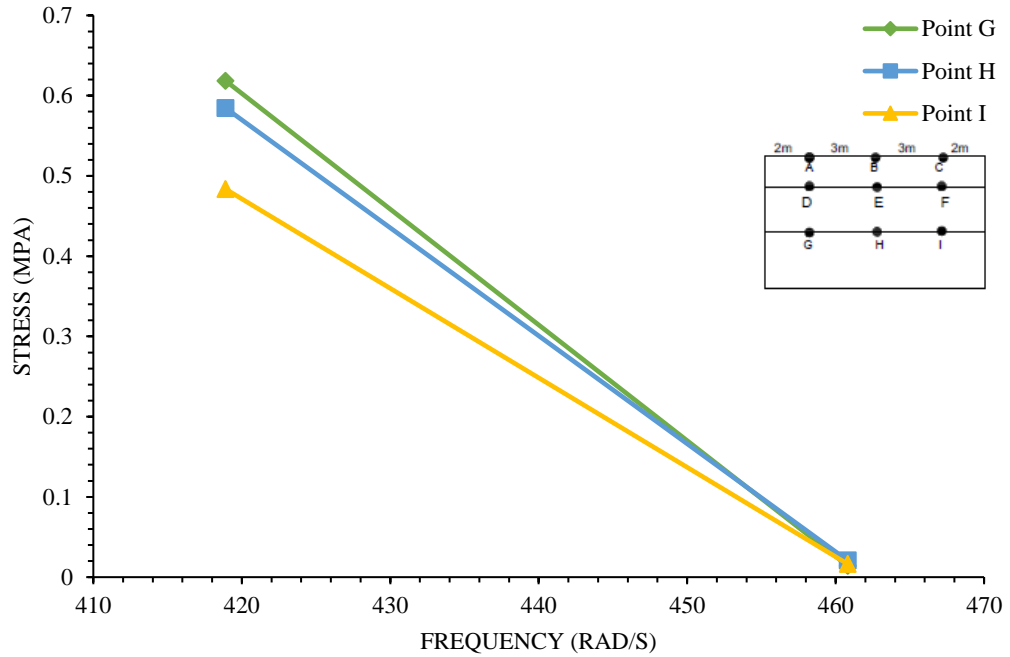


Figure 39 – Stress variation in subgrade layer for a vehicle load of 1600 kg

From Figures – 37 to 39, it is clear that as the frequency increased for gross vehicle weight of 1600 kg, the stress decreased. For the bitumen layer, at frequency 418.89 rad/s, the stress increases from 1.31 MPa at Point A to 3.23 MPa at Point B and then decreases to 1.82 MPa at Point C. For frequency 460.60 rad/s, the stress decreases from 0.042 MPa at Point A to 0.032 MPa at Point B and then increases to 0.043 MPa at Point C. In the bitumen layer, as the frequency increased, the stress decreased, like at Point A, the stress decreased from 1.82 MPa to 0.042 MPa. For the subbase layer, the stress increased from Point D to E and then decreased at Point F. For frequency 418.89 rad/s, the stress increases from 2.09 MPa to 2.30 MPa and then decreases to 1.64 MPa. And for frequency 460.60 rad/s, the stress increases from 0.050 MPa to 0.060 MPa and then decreases to 0.048 MPa. In the subbase layer too, the stress decreases at every point with increases in frequency. For the subgrade layer, at frequency 418.89 rad/s, the stress decreases from Point G to I, that is, the stress decreases from 0.618 MPa at Point G to 0.584 MPa at Point H and then further decreases to 0.483 MPa at Point I. And for frequency 460.60 rad/s, the stress increases from 0.014 MPa at Point G to 0.020 MPa at Point H and then decreases to 0.016 MPa at Point I. As the pavement depth increases, at points A, D, and G, the stress increases and then decreases from bitumen to the subgrade layer. On the other hand, the stress decreases at other points from the bitumen to the subgrade layer.

4.3 Pavement roughness

Figure – 41 shows the graph for variation of wavelength at different frequencies with respect to speed.

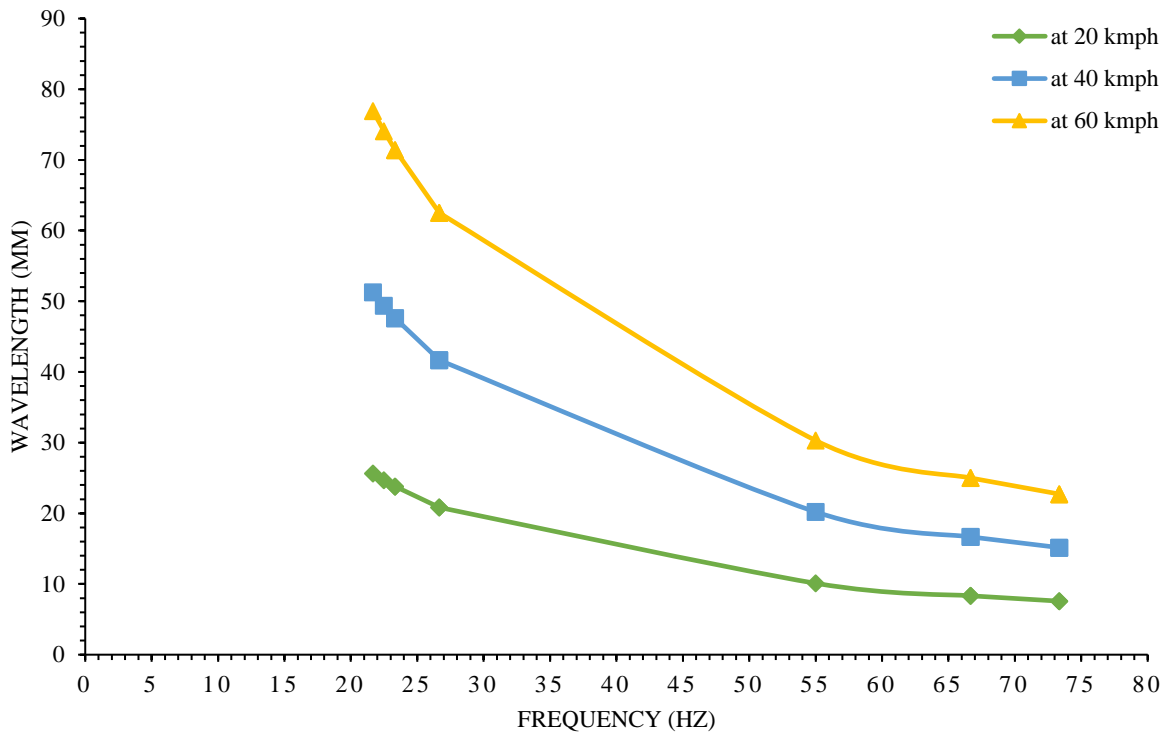


Figure 40 - Wavelength of pavement roughness at a different velocity

From Figure – 40, it can infer that when the RPM value is converted to frequency and then from it when the wavelength of pavement roughness is calculated, as the frequency increases, the wavelength of pavement roughness for a particular speed decrease. But for the same frequency, at different velocities, the wavelength of pavement roughness increases with increasing velocity. At velocity 20 kmph, the wavelength of pavement roughness decreases from 25.631 mm at 24.67 Hz to 7.575 mm at 73.34 Hz. Also, for a vehicle having a frequency of 21.67 Hz, the wavelength of pavement roughness increases from 25.631 mm at 20 kmph to 51.274 mm at 40 kmph to 76.911 mm at 60 kmph. At the same frequency, the velocity and wavelength of pavement roughness are directly proportional and for the same velocity and different frequency, the relation is inversely proportional.

CHAPTER – 5

CONCLUSION AND FUTURE RECOMMENDATION

5.1 Conclusion

From the present study, the following conclusions are drawn –

1. For the velocity variation of 20 to 60 kmph, the maximum residual stress was observed to be 18.25 to 55.32 kPa in the bitumen layer.
2. The decrease in stress was observed in the subbase layer along the pavement length for the velocity of 20 kmph and attained a constant value of 36.87 to 55.32 kPa for the velocity of 40 to 60 kmph. The stress increased from mid to end length of the pavement for 20 kmph velocity but decreased for 40 to 60 kmph velocity.
3. The stress increased from initial to mid pavement length and then decreased towards the pavement end length for 20 kmph velocity in the subgrade layer. But for velocities 40 to 60 kmph, the stress decreased along the pavement length.
4. For frequency of 21.67 to 73.34 Hz, the stress decreased from 200.73 to 1.31 MPa. This was due to change in the vehicle gross domestic weight and axle configuration.
5. For low gross vehicle weight, the stress increased from initial to mid pavement length and then decreased towards the end of the pavement length for frequency of 55 to 73.34 Hz. But as the load increased, the stress increased along the pavement length for frequency of 21.67 to 26.67 Hz.
6. For the frequency of 21.67 to 73.34 Hz, the wavelength of pavement roughness decreased from 25.631 to 7.575 mm for 20 kmph, 51.274 to 15.150 mm for 40 kmph and 76.911 to 22.725 mm for 60 kmph.

5.2 Future scope

This study does not consider the variation of displacement and acceleration due to changes in frequency, load, and velocity. Hence, numerical analysis in the future can be carried out to study the displacement and acceleration variation in the pavement. This study considered only the changing velocity, frequency, and load

but the study can be carried out by changing the pavement profile and its properties according to the site conditions. A study undertaking the settlement or deformation too can be carried out under the effect of load, velocity, and frequency.

References

1. Abaqus, V., 2016. 6.14, Online Documentation Help, Theory manual: Dassault Systems.
2. Assogba, O.C., Tan, Y., Sun, Z., Lushinga, N. and Bin, Z., 2021. Effect of vehicle speed and overload on the dynamic response of semi-rigid base asphalt pavement. *Road Materials and Pavement Design*, 22(3):572-602.
3. Al-Qadi, I.L., Xie, W. and Elseifi, M.A., 2008. Frequency determination from vehicular loading time pulse to predict appropriate complex modulus in MEPDG. *Asphalt Paving Technology-Proceedings*, 77, p.739.
4. Assogba, O.C., Sun, Z., Tan, Y., Nonde, L. and Bin, Z., 2020. Finite-element simulation of instrumented asphalt pavement response under moving vehicular load. *International Journal of Geomechanics*, 20(3), p.04020006.
5. Barbosa, R.S., 2011. Vehicle dynamic response due to pavement roughness. *Journal of the Brazilian Society of Mechanical Sciences and Engineering*, 33:302-307.
6. Beskou, N.D. and Theodorakopoulos, D.D., 2011. Dynamic effects of moving loads on road pavements: a review. *Soil Dynamics and Earthquake Engineering*, 31(4):547-567.
7. Bhavikatti, S.S., 2005. Finite element analysis. New Age International.
8. Das, B.M., 1983. Fundamentals of soil dynamics (No. Sirsi) i9780444007056).
9. Dhatt, G., Lefrançois, E. and Touzot, G., 2012. Finite element method. John Wiley & Sons.
10. Gao, J., 2020, May. Asphalt Pavement Stress Intensity Analysis under Fluctuating Load. In *IOP Conference Series: Earth and Environmental Science* (Vol. 508, No. 1, p. 012217). IOP Publishing.
11. Gao, J., 2020, May. Asphalt Pavement Stress Intensity Analysis under Fluctuating Load. In *IOP Conference Series: Earth and Environmental Science* (Vol. 508, No. 1, p. 012217). IOP Publishing.
12. Goenaga, B., Fuentes, L. and Mora, O., 2019. A practical approach to incorporate roughness-induced dynamic loads in pavement design and performance prediction. *Arabian Journal for Science and Engineering*, 44(5):4339-4348.
13. Hadi, M.N. and Bodhinayake, B.C., 2003. Non-linear finite element analysis of flexible pavements. *Advances in Engineering Software*, 34(11-12):657-662.

14. Hardy, M.S.A. and Cebon, D., 1994. Importance of speed and frequency in flexible pavement response. *Journal of Engineering Mechanics*, 120(3):463-482.
15. Hughes, T.J., 2012. *The finite element method: linear static and dynamic finite element analysis*. Courier Corporation.
16. IRC 6:2014, *Standard specifications and code of practice for road bridges, Section: II Loads and stresses*
17. IRC 37:2018, *Guidelines for the design of flexible pavements, fourth revision*
18. Jianhong, G., Youjun, X. and Shengchun, Y., 2020. Driving Direction Displacement Analysis of Asphalt Pavement under Fluctuating Load. In *E3S Web of Conferences* (Vol. 165, p. 03043). EDP Sciences.
19. Kadela, M., 2016. Model of multiple-layer pavement structure-subsoil system. *Bulletin of the Polish Academy of Sciences. Technical Sciences*, 64(4):751-762.
20. Kim, S.M., Rhee, S.K., Park, H.B. and Yun, D.J., 2009. Correlations among pavement surface roughness, moving dynamic vehicle loads, and concrete pavement performance. In *Performance Modeling and Evaluation of Pavement Systems and Materials: Selected Papers from the 2009 GeoHunan International Conference* (pp. 25-31).
21. Khavassefat, P., 2014. *Vehicle-Pavement Interaction* (Doctoral dissertation, KTH Royal Institute of Technology).
22. Khanna, S.K. and Justo, C.E.G., 1991. *Highway engineering*. Nem Chand & Bros.
23. Li, H., Wang, G., Qin, L., Wang, Q. and Wang, X., 2020. A spectral analysis of the dynamic frequency characteristics of asphalt pavement under live vehicle loading. *Road Materials and Pavement Design*, 21(2):486-499.
24. Lu, Z. and Yao, H., 2013. Effects of the dynamic vehicle-road interaction on the pavement vibration due to road traffic. *Journal of Vibroengineering*, 15(3):1291-1301.
25. Mulungye, R.M., Owende, P.M.O. and Mellon, K., 2007. Finite element modelling of flexible pavements on soft soil subgrades. *Materials & design*, 28(3):739-756.
26. Mikhail, M.Y. and Mamlouk, M.S., 1997. Effect of vehicle-pavement interaction on pavement response. *Transportation research record*, 1570(1):78-88.
27. Park, D.W., Papagiannakis, A.T. and Kim, I.T., 2014. Analysis of dynamic vehicle loads using vehicle pavement interaction model. *KSCE Journal of Civil Engineering*, 18(7):2085-2092.

28. Rahman, M.T., Mahmud, K. and Ahsan, S., 2011. Stress-strain characteristics of flexible pavement using finite element analysis. *International Journal of Civil & Structural Engineering*, 2(1):233-240.
29. Ranjan, G. and Rao, A.S.R., 2007. *Basic and applied soil mechanics*. New Age International.
30. Siddharthan, R.V., Krishnamenon, N., El-Mously, M. and Sebaaly, P.E., 2002. Validation of a pavement response model using full-scale field tests. *International Journal of Pavement Engineering*, 3(2):85-93.
31. Sukumaran, B., Willis, M. and Chamala, N., 2005. Three dimensional finite element modeling of flexible pavements. In *Advances in Pavement Engineering* (pp. 1-12).
32. Tang, F., Ma, T., Guan, Y. and Zhang, Z., 2020. Parametric modeling and structure verification of asphalt pavement based on BIM-ABAQUS. *Automation in Construction*, 111, p.103066.
33. Uddin, W., Zhang, D. and Fernandez, F., 1994. Finite element simulation of pavement discontinuities and dynamic load response. *Transportation research record*, (1448).
34. Wang, H., Zhao, J., Hu, X. and Zhang, X., 2020. Flexible pavement response analysis under dynamic loading at different vehicle speeds and pavement surface roughness conditions. *Journal of Transportation Engineering, Part B: Pavements*, 146(3), p.04020040.
35. Wu, J., Liang, J. and Adhikari, S., 2014. Dynamic response of concrete pavement structure with asphalt isolating layer under moving loads. *Journal of Traffic and Transportation Engineering (English Edition)*, 1(6):439-447.
36. Zhao, J. and Wang, H., 2020. Dynamic pavement response analysis under moving truckloads with random amplitudes. *Journal of Transportation Engineering, Part B: Pavements*, 146(2), p.04020020.